DEVELOPMENTS ON PHOTOACOUSTIC SPECTROSCOPY FOR TRACE GAS DETECTION OF AMMONIA VOLATILIZED FROM NITROGEN FERTILIZER

MILTON BAPTISTA FILHO

UNIVERSIDADE ESTADUAL DO NORTE FLUMINENSE DARCY RIBEIRO - UENF

CAMPOS DOS GOYTACAZES - RJ

FEVEREIRO DE 2011

DEVELOPMENTS ON PHOTOACOUSTIC SPECTROSCOPY FOR TRACE GAS DETECTION OF AMMONIA VOLATILIZED FROM NITROGEN FERTILIZER

MILTON BAPTISTA FILHO

"Tese apresentada ao Centro de Ciência e Tecnologia da Universidade Estadual do Norte Fluminense, como parte das exigências para obtenção do título de Doutor em Ciências Naturais"

Orientador: Prof. Dr. Marcelo Gomes da Silva

CAMPOS DOS GOYTACAZES - RJ

FEVEREIRO DE 2011

FICHA CATALOGRÁFICA

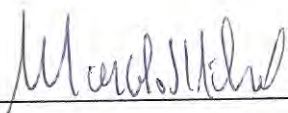Preparada pela Biblioteca do **CCT / UENF**   **06/2011**

DEVELOPMENTS ON PHOTOACOUSTIC SPECTROSCOPY FOR TRACE GAS DETECTION OF AMMONIA VOLATILIZED FROM NITROGEN FERTILIZER

MILTON BAPTISTA FILHO
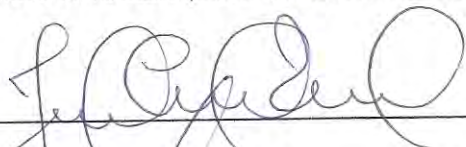
"Tese apresentada ao Centro de Ciência e Tecnologia da Universidade Estadual do Norte Fluminense, como parte das exigências para obtenção do título de Doutor em Ciências Naturais"

Aprovada em 15 de Fevereiro de 2011
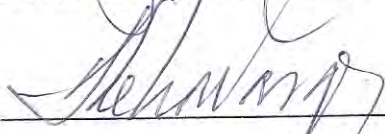
Comissão Examinadora:

_____
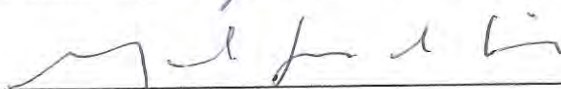
Prof. Marcelo Silva Sthel (Doutor, Física da Matéria Condensada)- UENF

_____

Dr. José Carlos Polidoro (Doutor, Agronomia - Ciência do Solo) - Embrapa Solos

_____

Prof. Helion Vargas (Doutor, Física da Matéria Condensada) - UENF

_____

Prof. Marcelo Gomes da Silva (Doutor, Física da Matéria Condensada) - UENF

(Orientador)

ii

Dedicatória

À todos que perseguem a realização de seus sonhos, lutam por seus ideais e são apaixonados pelos desafios que o caminho da vida lhes apresenta.

AGRADECIMENTOS

Ao Deus, por toda sua obra,

Aos meus pais, Milton e Sandra, que sempre me apoiar e me dar condições para chegar até aqui,

Aos meus irmãos, Silayne, Maurício, Sílvia e Messias, por me aguentar durante todos esses anos,

Aos meus avós, que quando em vida sempre valorizaram meu potencial, e de quem sinto muita falta,

À Thaís (a princesa do Marcelinho), pelo amor, carinho, paciência, inspiração, amizade e companheirismo que tanto me ajudaram na finalização desta etapa, e à Telma e família, por me receber com tanto respeito e carinho,

Aos Engenheiros Rennan e Jorge, pela amizade e de quem muito me orgulho de poder ter compartilhado o mesmo teto por tanto tempo de onde obtive muita sabedoria e amizade, e que são para mim irmãos,

Aos professores Marcelo Gomes da Silva, Marcelo Silva Sthel e Helion Vargas pela oportunidade e incentivo desde a iniciação científica,

Aos professores Fernando Souza Barros, Marisa Monte e José Carlos Polidoro pela colaboração no desenvolvimento do projeto,

Ao professor Marcelo de Oliveira Souza, pelas aulas durante a graduação e principalmente pelo seu maior ensinamento:a luta por dignidade e justiça,

Aos amigos Milena, Vanessa e Francisco pelo companheirismo, amizade e juntos formamos a inesquecível e revolucionária turma " *sub judice*",

Aos técnicos do Laboratório de Ciências Físicas, Luiz Antonio e Israel Esquef pela infinita boa vontade e ajuda fundamental no ajuste, manuntenção e solução de problemas em todo o laboratório,

Aos amigos do Laboratório de Ciências Físicas, em especial, Luisa, Francisco ("cadê chiquim?", Agora "Doutor Chiquim"), Léo, Anderson (LMGV), Gustavo (Gutim "Pleu-Pleu") e Wily ("Rapaizzz"),

Table of Contents

List of Figures

List of Tables

Resumo

O desenvolvimento da espectroscopia fotoacústica para detecção de traços de gases, em especial, amônia e gases relacionados ao ciclo do nitrogênio, é apresentado nesta tese. A amônia é uma molécula de papel fundamental no ciclo do nitrogênio devido à sua relação de balanço com o amônio. O amônio participa ativamente no processo de nitrificação em vegetais. Seu desequilíbrio representa emissões de amônia ao ambiente levando a produção de aerosol e perdas econômicas para a agricultura. Por isso, o desenvolvimento de técnicas visando a detecção de traços de amônia a nível de partes-por-bilhão e milhão tem grande demanda em estudos relacionados a agricultura e sistemas microbiológicos. A espectroscopia fotoacústica, em particular baseada em lasers semicondutores, vêm apresentando ótimos resultados nos últimos vinte anos para detecção de traços de amônia quanto a seletividade, sensibilidade e resposta no tempo.

Neste sentido, o objetivo principal desta tese foi desenvolver e aplicar a espectroscopia fotoacústica para detecção de traços de amônia no estudo de zeólitas naturais sendo utilizadas como meio de aumentar o tempo de permanência de fertilizantes nitrogenados em solos tropicais. Tipicamente, solos tropicais, tais como encontrados em boa parte do território brasileiro, apresentam maior taxa de volatilização de amônia de uréia (um dos principais fertilizantes nitrogenados utilizados no Brasil) por várias razões, entre elas, alto volume de chuvas, temperatura média alta e pH desfavorável do solo. A aplicação da espectroscopia fotoacústica consistiu em monitorar a taxa de volatilização de amônia de sulfato de amônio misturado a zeólita natural em diferentes temperaturas. Rampas de temperatura nas amostras entre 25°C e 100°C também foram realizadas de forma consorciada ao monitoramento da taxa de volatilização de amônia.

Numa outra etapa, um laser diodo acoplado por fibra óptica foi utilizado para caracterizar e comparar a performance de duas células fotoacústicas diferenciais: a primeira com dimensões convencionais e outra no mesmo design da célula tradicional, porém com dimensões menores. Da segunda célula, espera-se obter vantagem quanto ao tempo de resposta do sistema e menor espaço demandado na montagem experimental. A comparação dos resultados obtidos mostrou que a performance da célula menor foi inferior à performance da célula tradi-

cional. Porém, a célula menor pode ser bem empregada em aplicações que demandam limite de detecção acima de partes-por-milhão.

Por fim, um sistema de modulação de dois lasers de cascata quântica e simultâneo foi empregado utilizando software e placa de aquisição de sinal analógico. Dois lasers de cascata quântica, o primeiro para excitação de moléculas de óxido nítrico em torno de $5.29\mu m$ e o outro, para excitação de moléculas de óxido nitroso em torno de $7.7\mu m$ foram utilizados. Os resultados encontrados mostraram que o sistema teve excelente seletividade e sensibilidade, caracterizando-se por um sistema com ótima performance para ser empregado em montagens experimentais para ser utilizadas num nível mais próximo à fonte de emissão de gases e mesmo mais próximo ao campo.

Palavras-chave: Amônia, Espectroscopia fotoacústica, laser de cascata quântica, Zeólita natural, traços de gases

Abstract

The development of Photoacoustic spectroscopy for trace gas detection, in special, for ammonia and gases involved in the nitrogen cycle, is presented in the thesis. Ammonia is a very important molecule for the nitrogen cycle due to its direct balance with ammonium. Ammonium act actively in the nitrification process of plants. Its unbalance represents releases of ammonia into the environment causing aerosol production an economic losses in the agriculture. Therefore, the development of spectroscopic techniques looking for ammonia trace detection in part-per-billion level has high demand for studies in agriculture and microbiological systems. Specially photoacoustic spectroscopy based on semiconductor lasers comes a great promise for ammonia trace gas detection in the last twenty years, particularly, because its selectivity, sensitivity and fast response.

In this sense, the main aim of this thesis was to develop and apply photoacoustic spectroscopy for ammonia traces detection in the study of natural zeolites as a way to increase the life time of nitrogen fertilizer in tropical soils. Typically, tropical soils, as in Brazilian territory, promote high urea volatilization (main nitrogen fertilizer used in Brazil) for several reasons, high rain volume, high median temperature and unfavorable pH of the soil. In this study, ammonia volatilized from natural zeolites samples, at different temperatures, after they were mixed in aqueous ammonium sulphate solution. The ammonia volatilization monitoring was carried out sweeping the temperature of the ammonium treated zeolites between 25^oC e 100^oC.

In another stage, diode laser coupled to optic fiber was used to caractherize and compare the performance of two differential photoacoustic cell: first, a conventional one and another, in the same design of the first one in smaller dimensions. For the second one, there was a expectation for faster response on the time and less demanded space in the experimental setup. The comparison has shown the performance of the smaller one was lower than traditional one. Anyway, the small cell can be proposed as an interesting system for some applications that do not demand lower level of detection, ofr instance, it can be used for detection in the range of parts-per-million.

Finally, a simultaneous modulation-demodulation system based on software and data acquisition card for two quantum cascade lasers was proposed and tested. Two quantum cascade lasers, the first one for nitric oxide molecules excitation around $5.29\mu m$ and, second one for nitrous oxide excitation around $7.7\mu m$ were applied. The results have shown the performance of the proposed system has clearly shown selectivity and sensitivity. Additionally, the system could be easily applied for experimental setups based on photoacoustic spectroscopy with more mobility to be set in the neighborhood of emission source and even directly in the field.

Keywords: Ammonia, photoacoustic spectrocopy, quantum cascade laser, natural zeolyte, trace gas detection

Chapter 1

Opening

1.1 Motivation

The anthropogenic emissions of different gases related to the nitrogen cycle, in special ammonia (NH_3)emissions, into the environment are quite significant for the unbalancing of the nitrogen cycle. In the agriculture, ammonia emissions are linked mainly to losses of fertilizers by volatilization and emissions from waste in livestock. In the first case, these losses contribute strongly for damage of the quality of air and eutrophication of lakes. Besides environmental damages, another problem caused by the losses of ammonia is the high cost involved in the production of large amount of nitrogen fertilizers.

Natural zeolites have been studied for waste treatment in different environmental applications. In agriculture, natural zeolites are interesting for treatment of waste from livestocks and reduce losses of nitrogen fertilizers, because the ability of some natural zeolites to retain ammonium (NH_4^+). Specially for nitrogen fertilizers, natural zeolites can act as a release controller. The kinetic of releasing can be drastically slowed down by the use of fertilizers in the soil when zeolites are mixed with fertilizer. Furthermore, natural zeolites are quite able to retain water in its structure, which is important water supply for plants.

In this sense, this work is intended to develop and use photoacoustic spectroscopy as a tool for monitoring the ammonia emission rate from natural zeolites mixed with nitrogen fertilizers. The determination of ammonia volatilization rate from natural zeolites is a fundamental step for the research of natural zeolites and fertilizers, which will be much useful for agronomists and microbiologists. Finally, we propose a system based on software and Data acquisition Card to modulate, demodulate and extract photoacoustic signal from a PA cell using two quantum cascade lasers simultaneously. This propose will be important to make a compact and portable

ammonia monitoring instrumentation.

1.2 Review on main subjects of the Thesis

1.2.1 Sensors for ammonia in gas phase

Ammonia detectors are demanded in different areas and in different level of sensitivity. Some examples are environmental emissions, automotive and chemical industry and medical applications. There are many methods for detecting ammonia disclosed in literature. For instance, from the simple use of type of detection in the exhaust pipe of vehicles to the sophisticated use environment ammonia monitoring. Most frequently used commercial ammonia detectors are metal-oxide gas sensors, catalytic ammonia detectors, conducting polymer ammonia analyzers and optical ammonia detection technique. Also, indirect systems using gas samplers and specific chemical reactions to make a selective ammonia analyzer are discussed in the literature [49].

Metal-oxide gas sensors have been manufactured on a large scale. They are based on metal-oxide films [54]. Owing to the fact that these sensors are rugged and inexpensive, they are promising for gas detection sensors. A common model is based on the fact that metal-oxide films consist of a large number of grains, contacting at their boundaries. The electrical behavior is controlled by the formation of double Schottky potential barriers at the interface of adjacent grains, caused by the different chemical potential between the interface. When exposed to a chemically reducing gas, like ammonia, co-adsorption and mutual interaction between the gas and the metal-oxide surface results in oxidation of the gas and change of the Schottky potential barrier [26, 46]. For instance, a typical lower ammonia detection limit is 1 parts-per-million (ppm), using WO_3 additives operated at an elevated temperature ($> 400^oC$) [53].

Catalytic ammonia sensors are based on the reactivity of catalytic metals with specific gases, like ammonia, hydrogen, carbon monoxide or organic vapours. The changes on the carrier concentration for the catalytic metal is influenced by a change in concentration of the gas. A field effect device sense the change in charge carriers. The selectivity of these sensors is related to the catalytic metal, the morphology and the operating temperature. The lower limit detection of such type of sensor is typically in the low-ppm range [34, 35, 52].

Polymers are also used as material for sensor device due to the changes of their electrical conductivity when exposed to gas. The sensing mechanism is based on reaction between sample

gas and polymer. The reduction of the polymer film provides a change in the conductivity of the material. This process makes the polymer film a suitable material for resistometric or amperometric ammonia detection. The lower detection limit of such devices is about 1 ppm. [30, 31, 32].

Ammonia optical gas analyzers are based on two principles. A chemical reaction of ammonia in solution changes its pH that could be determined by pH paper. A second process of ammonia detection is accomplished by coloring of a solution by ammonia. More sensitive performance of this method is achieved when photon-counting optical sensor is employed (sensitivity in parts-per-trillion range for ammonia detectors) [50].

The advent of the laser made breakthrough in spectroscopy, which made a great expanding for many areas. The first applications included detection of chemical molecules in air. Absorption and scaterring of the laser light are the main physical principle used for the trace gas detection. Up to now, various diagnostic methods based on physical process caused by laser light-environmental species are developed. Ideally, the main characteristics required for detecting and monitoring laser based spectroscopy technique are [47]:

- *High selectivity*, for a particular gas species, with no observable cross-response from other species; to measure accurately trace gas concentrations of less than a part per billion;

- *High sensitivity, to detect a very low concentration, below ppt (parts-per-trillion, 10^{-12});*

- Possibility to detect numerous compounds with one instrument;

- Special for the photoacoustic spectroscopy, wide dynamic range to monitor high and low concentrations with a single instrument, in a real-time response that can be linear over more than four decades of concentration;

- Fast response, with measurement speeds of fractions of a second, or signal averaging to achieve still higher sensitivity;

- Good temporal resolution for on-line monitoring;

- Noninvasiveness and nondestructiveness, which do not disturb the sample under analysis.

Optical absorption spectroscopy is used in the most sensitive and selective ammonia detectors for environmental ammonia. In gas detection process, the spectrum of the light reaching the detector is influenced by the gas composition. These systems are used in all kind of gas analyzers in different application areas. Optical absorbance analyzers that measure multiple gases

are commercially available, but there are some drawback: they are expensive and sensitivity of absorption is partly determined by the amount of gas between the light source and the detector. Thus, miniaturization always results in an increase in the lower detection limit [49].

1.2.2 Photoacoustic Spectroscopy (PAS)

Many attentions has been given to the trace gas detection the last two decades because of the great demand of sensors to assess environmental problems related to agriculture, biology, engineering and industry [28, 51]. Trace gas sensors with good selectivity, good sensitivity, fast answer, compactness and mechanically resistance are a permanent task for trace gas sensors research. In the middle of different spectroscopic techniques, the photoacoustic spectroscopy (PAS) has shown several advantages in relation to the other techniques as good selectivity, low costs, reasonable sensitivity, compactness and fast answer [36]. The PAS has presented good sensitivity for different molecules like carbon dioxide (CO_2), ammonia (NH_3), ethylene (C_2H_4), nitrous oxide (N_2O), NO_x, methane (CH_4), etc.

The performance of PAS has been improved recently with the introduction of modern laser sources as quantum cascade lasers (QCL), multi quantum well diode lasers [10, 21], non-linear optimization (OPO, OPA) [8] and design of different geometries of the sensor [36]. Focusing in solid-state lasers, they have the main advantage in the compactness, differently of the gas lasers that demand huge rooms and more energy. Those lasers are built to emit in different ranges in the near- and mid-infrared, especially diode lasers for telecommunications are built to emit at the near-infrared ($1550 \eta m$) where are found absorption coefficients of 10^{-6} cm^{-1} and 10^{-3} for ammonia and acetylene, respectively, for example [14, 39]. Quantum cascade lasers, which can be built to emit in the near and mid-infrared ($4 - 11 \mu m$) have also shown good performance for spectroscopic proposes. Reports in literature have shown low limit detection for molecules like ammonia, ethylene, NO_x and nitrous oxide using PAS and quantum cascade laser in the level of dozens of parts per billion. Nowadays, DFB[1] diode lasers have gained more attention because their low cost and improvements for output power.

The generation of the Photoacoustic Effect in trace of gases is based on the absorption of near and mid-infrared light. Such absorption is known because they excite rotational and vibrational modes on the structure of some small molecules. These modes are quantized and are quite specific for each molecule as a *fingerprint*. The absorption of photons results in the excitation of molecular energy levels (rotational, vibrational and electronic). The excited state

---

[1]Distributed Feedback

losses its energy by radiation process, such as spontaneous or stimulated emission, and/or by collisional, in which the energy is transformed into translational energy [36].

For vibrational excitation, radiative emission and chemical reactions do not play an important role, because the radiative lifetime of vibrational levels are long compared with the time needed for collisional deactivation at pressures used in photoacoustics and the photon energy is too small to induce chemical reactions. Thus, in practice the absorbed energy is completely released as heat, appearing as translational (kinetic) energy of the gas molecules. The deposited heat power density is proportional to the absorption coefficient and the incident light intensity [36].
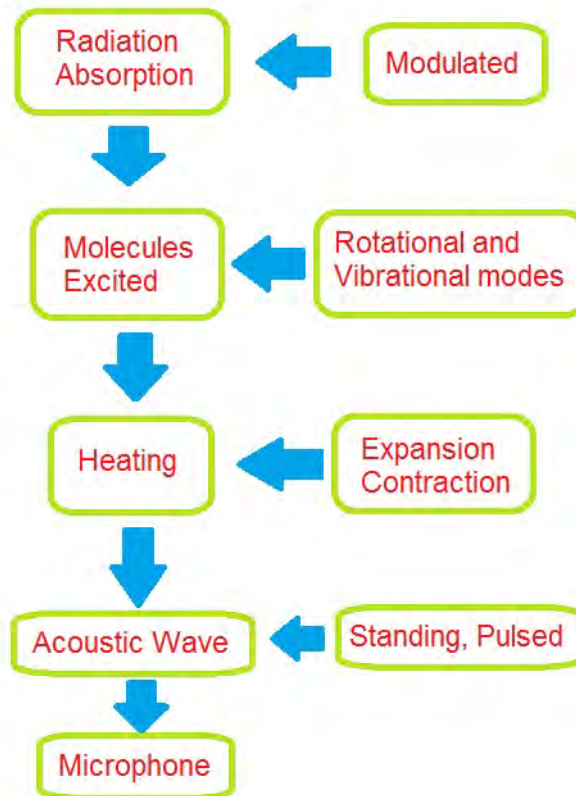
Figure 1.1: Diagram for the Photoacoustic Effect [36].

In the figure 1.1 are summarized the steps for the PA effect concept and further detection of acoustic waves by microphone. The electric signal generated from the polarized microphone used to be in the range of μV and ηV, is also modulated in the same frequency of the laser source, which is the radiation used to excite the molecules. This single frequency is singled out from the microphone signal and amplified and, the other frequencies, that are buried in noise, are rejected. Normally, such task is made in a *lock in* amplifier.

A conventional photoacoustic spectrometer consists of a radiation source, a modulator, a photoacoustic cell and a signal acquisition and processing equipment. Figure 1.2 present a schematic diagram. The modulated laser radiation passes through the PA cell filled with the gaseous sample and enters a power monitor. The absorption of modulated light generates an acoustic signal in the cell, used for photoacoustic measurements. The PA signal can be amplified by tuning the modulation frequency to one of the acoustic resonances of the sample cell. In this resonant case the cell works as an acoustic amplifier; the absorbed laser power is accumulated in the acoustic mode of the resonator for Q oscillation periods, where Q is the quality factor, typically in the range of 10-300. The excited sound waves can be detected by an electret or condenser microphone and the microphone signal is measured by a *lock-in* amplifier [13].
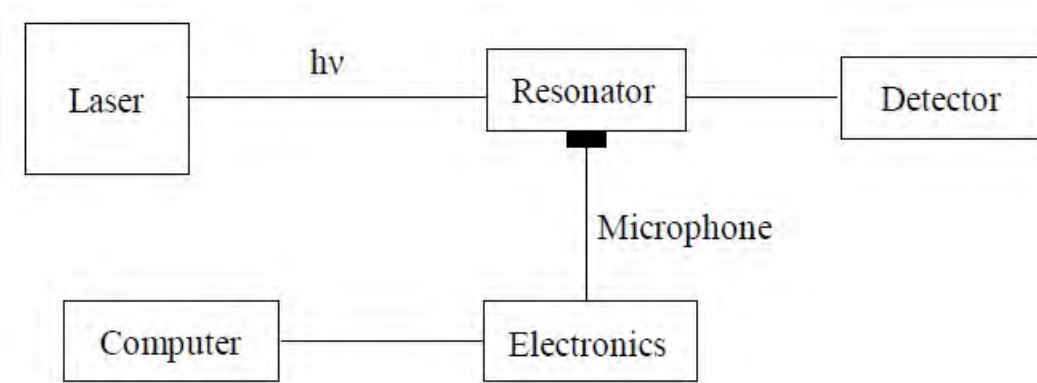
Figure 1.2: Typical PA spectrometer [13]

The PAS is an infrared spectroscopy technique based on the absorption of the light and consequently generation of heat followed by generation of sound waves. These sound waves are detected by a microphone. The signal generated in the microphone (Equation 1.1) is proportional to the concentration of gas (c) and absorption coefficient of the molecule (α), Q factor of the sensor, the intensity of the laser in the specific wavelength ($I(\lambda)$) and the modulation frequency of laser (F). The measurements run in continuous gas flow which characterizes the real time measurement.

$$PA_{\text{Signal}} = C(F).\Sigma a_i.c_i.I(\lambda) \qquad (1.1)$$

The equation 1.1 has a linear regime for low concentrations (based on the absorption saturation). Based on the equation 1.1, the concentration of gas (c) can be determined. Mixtures of gas can be expressed with a series of sum of the terms α_i and c_i in that equation, where i represents 1, 2,..., n molecules in the system that can absorb at the λ_i. Improvements in the

sensitivity are possible increasing directly the intensity of the source and the acoustic amplification of the sensor. C(F) is the setup constant, which defines the sensitivity of a PA resonator to the pressure at the resonance frequency F [36]. It depends mainly on spatial dimensions, Q factor and position of the microphone on the resonator tube and sensitivity of the microphone [45]. Setup constant can be determined from PA signal, features of microphone and absorption coefficient of the molecule according to the equation 1.2 [42]:

$$C(F) = \frac{S_c}{S_m.P.\alpha} \tag{1.2}$$

S_c is the PA signal for a generic concentration in the range what is intending to measure (respecting such limit of the linearity of Lambert-Beer Law). S_m is the sensitivity of the microphone at the frequency of resonance; P is the output power of the laser and α is the absorption coefficient for the molecule at such (c) concentration. To compare different PA cells demands to know more generic features as the minimum absorption coefficient (α_{min}), as the minimum concentration limit (c_{min}) and the sensitivity of the setup (D_{PA}). Based on the background signal and its standard deviation, it could be define the minimum PA signal (S_{min}) what the system is suppose to detect as it takes account Signal-to-Noise-Ratio = 1 (Equation 1.3):

$$S_{min} = S_{Background} + \sigma_{Background} \tag{1.3}$$

As it would define the α_{min},

$$\alpha_{\min} = S_{\min}/C.P \tag{1.4}$$

And c_{min},

$$c_{min} = c.S_{\min}/S_c \tag{1.5}$$

D_{PA} is a generic parameter that depends on the output power of the laser:

$$D_{PA} = \alpha_{min}.P \tag{1.6}$$

Photoacoustic spectroscopy is ideally a background-free technique, since the signal is generated only by the absorbing gas. However, background signals can originate from nonselective absorption of the gas cell windows (coherent noise) and external acoustic (incoherent) noise [13]. A differential cell (1.3) was specifically designed [37] for fast time response, low acoustic and electric noise characteristics and high sensitivity. In order to reduce the flow noise and

external electromagnetic disturbances a fully symmetrical design was developed. Two resonant acoustic cells (5.5 mm diameter tubes) were placed between two acoustic filters (C and F in figure 4.3). The gas flow passes through both tubes, producing about the same flow noise in both resonator tubes. However, the laser light irradiates only one of them, thus the PA signal is generated in only one tube. Each tube has a microphone embedded at middle of each one and the difference of their signals is amplified by a differential amplifier. Such signal generation procedure can reject flow noise and window coherent noise [37].
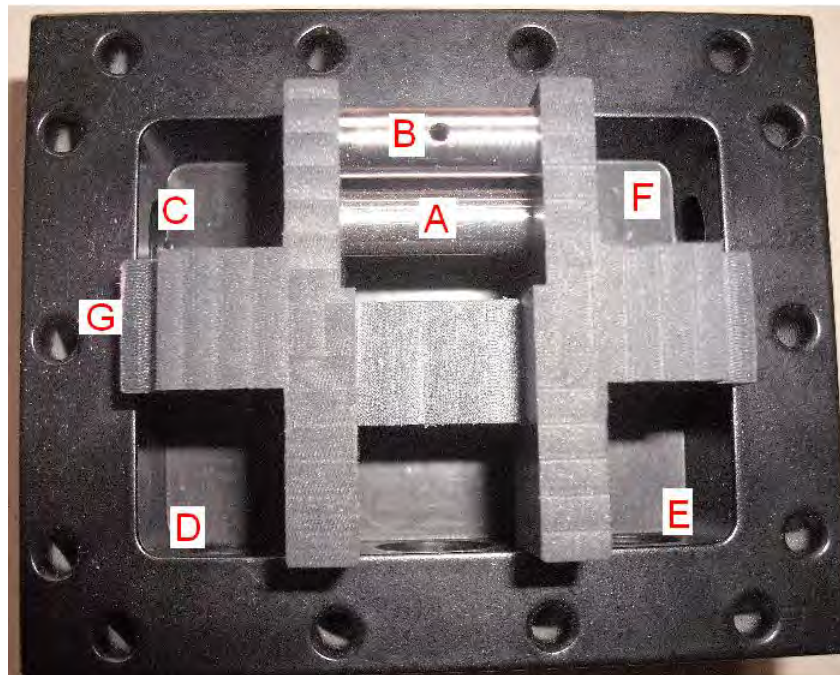
Figure 1.3: Internal schematic of Differential PA cell.In the figure, two resonant tubes are placed in A and B. C and F indicate where are two of four buffers. D and E are the in- and outlets. G represents one of two ways for gas flow between buffers.

1.2.3 Semiconductor laser sources

The necessary sensitivity and selectivity can be achieve by the uses of high-resolution laser techniques in the infrared (IR) and near-infrared (NIR) fingerprint regions. In fact the availability of tunable laser sources with suitable linewidths is essential for the further development of optical diagnostic techniques already well established in trace-gas analysis [18, 45].

The radiation sources for sensitive and selective PAS applications must exhibit the following characteristics: 1) high optical power, 2) narrow linewidth, 3) single mode operation, 4) low source noise and low amplitude fluctuations, 5) high stability and reliability, 6) compact and

robust overall sensor package [10]. In this respect, single-mode distributed-feedback (DFB) $AlGaAs$ diode lasers with their high spectral resolution are ideally suited for detecting chemical bonds such as N-H, O-H, and C-H. These versatile NIR lasers work at near room temperature, are robust, have low-cost, and are portable detection of trace gases [6].

The operating principle of diode lasers (semicondcutor lasers) involves electrons and holes recombination followed by giving off laser photons, which wavelength is close to the bandgap of the active region of the semiconductor. Its available to build diode lasers emitting at different wavelengths. On the other hand, the operation of the Quantum Cascade Laser (QCL) is independent of the bandgap. Instead of using pair recombination, QCLs use only one type of charge carrier (electrons) that undergoes quantum jumps between energy levels E_n and E_{n-1} to create a laser photon of frequency ($\frac{E_n - E_{n-1}}{h}$). The photon frequency is determined by structuring the active region in ultra-thin layers known as quantum wells of nanometric thickness. The state of electrons moving perpendicular to the layer interfaces is quantized and characterized by the thickness of the wells and by the height of the energy barriers [10].

Currently available DFB quantum cascade lasers (QCL) makes the IR accessible, where the absorption coefficients are 1-2 orders of magnitude higher. These lasers can be operated in pulsed mode near room temperature or in continuous-wave (cw) mode reach power levels comparable with those of DFB diode lasers (1-50 mW) [45]. QCLs are characterized by a limited tuning range: either approximately 3-4 cm^{-1} by adjusting the injection current or up to approximately 10 cm^{-1} by controlling the temperature of the laser chip [13].

As the PA signal is directly proportional to the laser power, the Amplitude Modulation (AM) is based on sinusoidal lightening of the gas (State ON and OFF on the time). Wavelength Modulation (WM) scheme conventionally describes the case where the modulation frequency is much less than the width of the spectral feature of interest and the modulation index is high. Generally, this corresponds to modulation frequencies from a few kilohertz to a few megahertz. Semiconductor lasers can be easily and rapidly modulated, through a modulation of their injection current. Laser modulation capability is a key issue for high sensitivity gas detection and many of the most performant techniques for trace gas monitoring take advantage of laser modulation for noise reduction and high sensitivity detection [13].

1.2.4   Natural zeolite as carrier of fertilizers

Zeolites are hydrated alumninosilicates, characterized by three-dimensional networks of SiO_4 and AlO_4 tetrahedra, linked by the sharing of all oxygen atoms. The partial substitution

of Si^{4+} by Al^{3+} results in an excess of negative charge which is compensated by alkali and earth alkaline cations. These cations are located along with the water molecules in cavities and channels inside the aluminosilicate macroanion framework. The water molecules can be reversibly removed or replaced by other sorbates [44].

Zeolites are capable of sorbing into their cavities or channels different polar and non-polar inorganic or organic molecules but also biochemically, pharmaceutically, agrochemically effective compounds, odoriferous compounds and others. In agriculture the natural zeolites are widely used as slow releasing carriers of fertilizers [41, 44]. Zeolites added to fertilizers help to retain nutrients and, therefore, improving the long term soil quality by enhancing its absorption ability. Zeolites can retain nutrients in the root zone used by plants when required. Consequently this leads to more efficient use of fertilizers by reducing their rates for the same yield, by prolonging their activity of finally by producing higher agriculture yields. Large losses of fertilizers which move out of the root zone (leaching) often happen in sandy soils, which lose their capability to retain high nutrient levels. Therefore an application of zeolites will enhance the plant growth and development by reducing the loss of nutrients [41].

Natural zeolites are suitable carriers for fertilizers of various kinds. The nutrients are released gradually. Very important is also the hydratation and dehydratation capacity of zeolites which may be used to improve the water balance in the soil. Zeolite based fertilizer has several advantages: it is a fertilizer prepared on the base of a non-toxic natural material, it is easily applied at the beginning of the vegetation period that supplies an even fertilizing effect throughout the whole period. It is ecologically advantageous since the active compounds and nutrients are washed out into the soil slowly and gradually. In case of torrential rains they are not washed out all at once and thus there is no underwater pollution or the pollutation of neighboring rivers [44].

1.3   Body of the Thesis

This thesis was developed on the experimental concepts of photoacoustic spectroscopy for ammonia trace gas detection. An experimental setup based on quantum cascade laser for ammonia traces detection that was mounted previously [3] was improved and the sample holder system prepared for receiving powder samples.

In the **Chapter** 2, measurements involving natural zeolites are described: first, monitoring of ammonia emission rate from three natural zeolites treated with an aqueous ammonium

sulphate solution at 30 and 60°C and second, monitoring of ammonia emission rate from two natural zeolites treated with an aqueous ammonium sulphate solution during a temperature ramp from 25 to $100^{o}C$.

Chapter 3 presents a performing comparison of two differential PA cells. The first one is a conventional model that was already exhaustively evaluated in [36, 37]. The second one is a smaller version of the conventional one. The comparison is made for ammonia trace detection and monitoring. At the end, some perspectives are figure out.

Chapter 4 presents results found for a Software-Based Lock-in (SBLI). This system was tested for ammonia absorption based on DFB diode laser. At the end, the system was proposed to work for two quantum cascade lasers, simultaneously and, its performance was evaluated.

Finally, we present some future directions that we collect from the work made in this Thesis (**Chapter** 5).

Chapter 2

Ammonia emission rate monitoring based on photoacoustic spectroscopy applied to fertilizers study

2.1 Introduction

It is no longer questioned that present-day agricultural practices play a significant role in the unbalancing of the nitrogen cycle, especially the widespread application of fertilizers, which results in plenty of nitrous oxide and ammonia outputs [25, 16, 40]. The great amounts of greenhouse gases like nitrous oxide and methane produced by agricultural activities have raised again the discussion on how to reduce extensive agricultural emission. Other environmental damages that are also related to the use of fertilizers are the pollution of fresh water reservoirs and the atmosphere, which result in eutrophication and air acidification, respectively. Furthermore, the demand for food is increasing rapidly, but the production of fertilizers does not follow with the same rate [9, 11]. Consequently, the improvement of efficient use of fertilizers can be a fundamental contribution for a sustainable large-scale agriculture [24, 48].

The extent of arable land is insufficient for the continued expansion of food production, but it is likely that South America can fulfill the promise of satisfying the increasing world demand for food. Brazil, for instance, has an enormous potential for food production and a large part of its economy is based on agricultural practices. Nevertheless, due to the heavy rain regime and high temperatures throughout the year, Brazilian soils are poor in nitrogen compounds. The uncontrolled use of large amounts of nitrogen fertilizer resulting in volatilization of ammonia is

wasteful and does not contribute to remedy these serious concerns. Alternatives to improving fertilizer lifetimes on the soil must be searched in order to render agriculture more economically sound and environmental friendly.

The speedy releasing process of fertilizers right after they are spread over the soil is one of the main causes of waste, which can happen by volatilization or by leaching. Therefore, the detailed knowledge of volatilization kinetics of the nitrogen containing compounds is fundamental for promoting the appropriate usage of fertilizers to provide nutrients for plants while avoiding excessive damage to the environment. It has been shown that minerals like clays and zeolites can be used to control the release of fertilizer onto soils, notably at low cost [17]. Furthermore, natural zeolites can readily exchange ions like ammonium, which is very important for plant feeding [44].

To evaluate and compare the ability of different zeolites to hold ammonium and increase the lifetime of nitrogen fertilizers, it is necessary to study the physical and chemical properties of such materials. Studies must focus on factors which are essential for controlling the ion exchange capacity with various nitrogen sources, such as ammonium sulphate and urea, in real time under conditions that reproduce closely those that will be found in the crop fields. Photoacoustic spectroscopy is a useful trace gas analysing technique. It is an infrared spectroscopy based technique that has typically very simple experimental setup. Their advantages are to be compact, to have simple operation, low cost and high selectivity, and it is highly sensitive. Photoacoustic spectroscopy in the mid-infrared range has nowadays important application in the detection of trace amounts of environmentally and biologically important gases such as methane, ammonia, nitrous oxide, ethylene, ozone, nitric oxide, etc [3, 29].

The beginning of PAS was in the 1970's, when the gas lasers (such as CO_2) have been increasingly used as radiation source because of their high power and broad discrete emission range. However this kind of radiation source demands laboratory space and its operation can be cumbersome. In the last few years numerous applications have been presented for new semiconductor lasers (DFB diode lasers, quantum cascade lasers) and optical parametric oscillators in photoacoustic spectroscopy. These sources of radiation operate typically with less power than gas lasers, but their reduced size, ease of operation, narrow and specific emission lines promise good results. As a consequence, recently many articles have shown impressive detection limits, as low as parts per billion, using such lasers in PAS [3, 29]. Nowadays, PAS is largely used for trace gas detection in many applications as industry, biological and agriculture systems study.

2.2 Ammonia traces detection based on Photoacoustic Spectrocopy for evaluating natural zeolites as kinetic fertilizer release controller

In this section, a study of chemical and physical properties, as well ammonia desorption features of zeolite materials is reported. Ammonium sulphate was used as nitrogen sources and three different zeolites were analyzed.

2.2.1 Material and Methods

Three microporous materials were used as ammonia holders: two natural zeolites from Cuba and Chile (furnished by Celta Brasil, Cotia, SP, Brasil) and a so-called zeolite concentrate (ZC), produced from a naturally occurring mixture of clays, zeolite and quartz extracted from central-northern Brazil [4, 38], provided by CETEM and CPRM (Rio de Janeiro Brazil).

Fundamentals

Photoacoustic Spectroscopy (PAS) is a spectroscopic technique based on the infrared region (near and mid-infrared, $1 - 11\mu m$). It is largely used to detect the emission of gases in trace levels. The absorption of infrared (IR) radiation by a molecule results in activation of higher-energy rotational-vibrational modes. Each mode of transition has a specific absorption energy value. Thus, a group of transitions gives for each molecule a typical absorption pattern, also called molecule fingerprint. The IR radiation is modulated at the resonance frequency of the photoacoustic cell (PA cell). During the relaxation, heat is transferred in the gas phase and pressure waves are generated by expansion, and detected by microphones, which is internally set in the PA cell [36]. The main advantages of PAS are the real time monitoring (continuous flow), low cost, high selectivity, good sensitivity (parts per billion), ease of operation, and the reduced size of the experimental apparatus.

Experimental Set-up

A schema of the experimental set-up is described in the figure 2.1. The source of excitation used was a quantum cascade laser [23], with emission wavenumber tunabled between 1045 and 1052 cm^{-1} by temperature setting. No significant water absorption is observed in this spectral range, but problems related to ammonia desorption from the PA cell walls induced by water
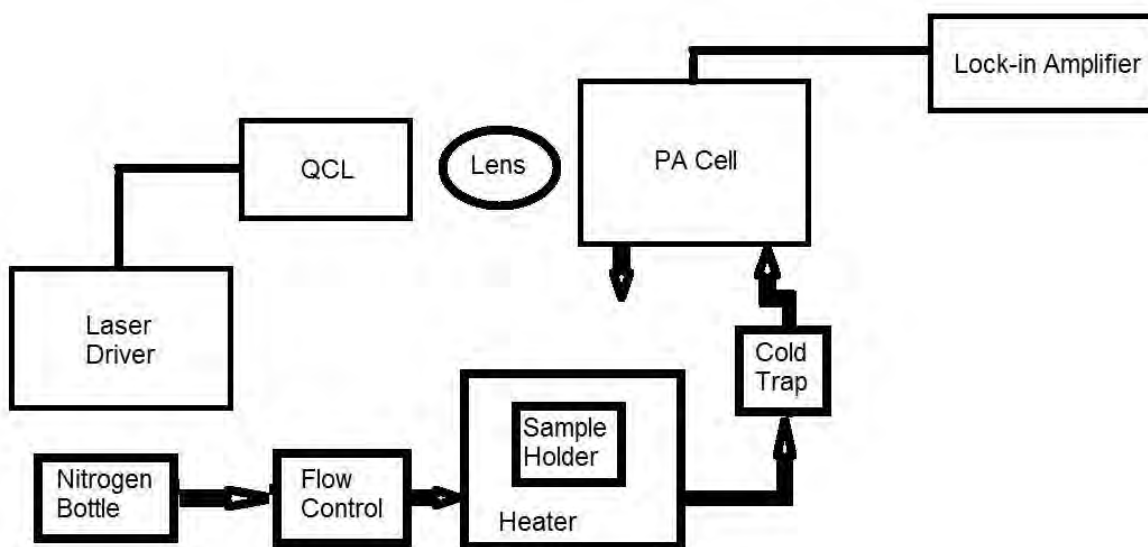
Figure 2.1: Experimental Setup.

adsorption led us to use a cold trap to remove water from the gas samples [4], what has no effective influence on the sensitivity and selectivity of the sensor. A lock-in amplifier (Stanford Research Systems, model SR850) was used to modulate the laser driver at the PA cell resonance frequency (3765 Hz) and to collect the signal from the microphones. A glass flask was used to hold the samples and a homemade heating system based on a peltier element (heating controller Novus 2000) was assembled at the bottom of the sample holder. Pure nitrogen (Praxair Inc., 99.95% purity) controlled by electronic flowmeters (Brooks S5650) was used as carrier gas and a flow of 5 $\frac{L}{h}$ was applied. The low detection limit of this setup was reported as 66 ppbV [3]. Room and near room temperature desorption was carried out setting the laser wavenumber at 1046.4 cm^{-1}, which corresponds to the strongest absorption line for ammonia. After signal saturation, the laser temperature varied between -20 and 35^oC, resulting in a wavelength scan from 1049 to 1046 cm^{-1}. This procedure was carried out in order to ensure that the signal at 1046.4 cm^{-1} (9.55μm) was due solely to ammonia molecules.

Preparation of the samples

Samples of each material were mixed (1250 mg of each material) in an ammonium sulphate aqueous solution ($\frac{7.2g}{L}$) (economically viable proportion) and stirred over a magnetic stirring plate for 3 h. Subsequently the materials were filtered using paper filter and 950 mg of the samples were added to the glass sample holder and their ammonia emission rates were

monitored by PA signal. Ammonia desorption was followed at two different temperatures, i.e., 30^oC and 60^oC and always at the same flow ($\frac{5L}{h}$).

2.2.2   Results and Discussion

The Figure 2.2.A and 2.2.B show the results of ammonia emission rate from the zeolite samples at 30 and 60^oC, respectively. At both temperatures the Cuban zeolite emits more ammonia than the ZC and the Chilean zeolite. At 30^oC, a mean ammonia desorption rate of 19.40 $\frac{\mu L}{h.g}$ (with a $\pm$ 2.31 $\frac{\mu L}{h.g}$ of standard deviation) was found for the Cuban zeolite and respectively values of 7.53 $\frac{\mu L}{h.g}$ and $\pm$ 0.22 $\frac{\mu L}{h.g}$ were obtained for the ZC samples. The amount of ammonia emitted from the Chilean zeolite is near to the limit of detection, i.e., 66 ppbV.

As expected, the ammonia desorption rate at 60^oC for each zeolite has increased. Typically, a mean value peak of 114 $\frac{\mu L}{h.g}$ (standard deviation = $\pm$ 11.7 $\frac{\mu L}{h.g}$) was obtained for the Cuban zeolite. The averange emission rate for the Chilean zeolite was found to be 7.09 $\frac{\mu L}{h.g}$, and that for the ZC reached 38.6 $\frac{\mu L}{h.g}$ (with $\pm$ 1.50 $\frac{\mu L}{h.g}$ and $\pm$ 2.02 $\frac{\mu L}{h.g}$ standard deviations, respectively). Consequently, in order to identify a correct application of each zeolite as fertilizer microporous carrier, it is important to take into account the demand for organic nitrogen of each cultivated species of plant. Therefore, as first indication, Cuban zeolite wasoutstanding as the best material to be used in crop yielding with high demand of nitrogen owing to its higher ability to hold and release ammonium at typical field temperatures.

Comparing the temperature effect on the desorption rates, a remarkable enhanced in intensity of desorption rate was observed for Chilean zeolite. While desorption rate for Cuban zeolite and ZC increased respectively by a factor of 6 and 5 as result of the temperature change from 30 to 60^oC, the ammonia desorption rate from Chilean samples increased by a factor of about 32. This indicates that an activation temperature higher than 30^oC is essential to promote desorption in Chilean zeolite. The fact of the increase ratio of ammonia emission rate for the ZC is close to that obtained for Cuban zeolite is also an indication that both zeolites have the same type of adsorption site.

After the desorption measurements at 30 and 60^oC the rest of organic nitrogen in the zeolite samples was determined by using of the total Kjeldahl nitrogen method. Table 2.1 summarize the results. Taking account the errors inherent to such quantification method, it is only plausible to point out that the remaining concentration of organic nitrogen in ZC is the half of the concentration estimated for Cuban and Chilean zeolites.
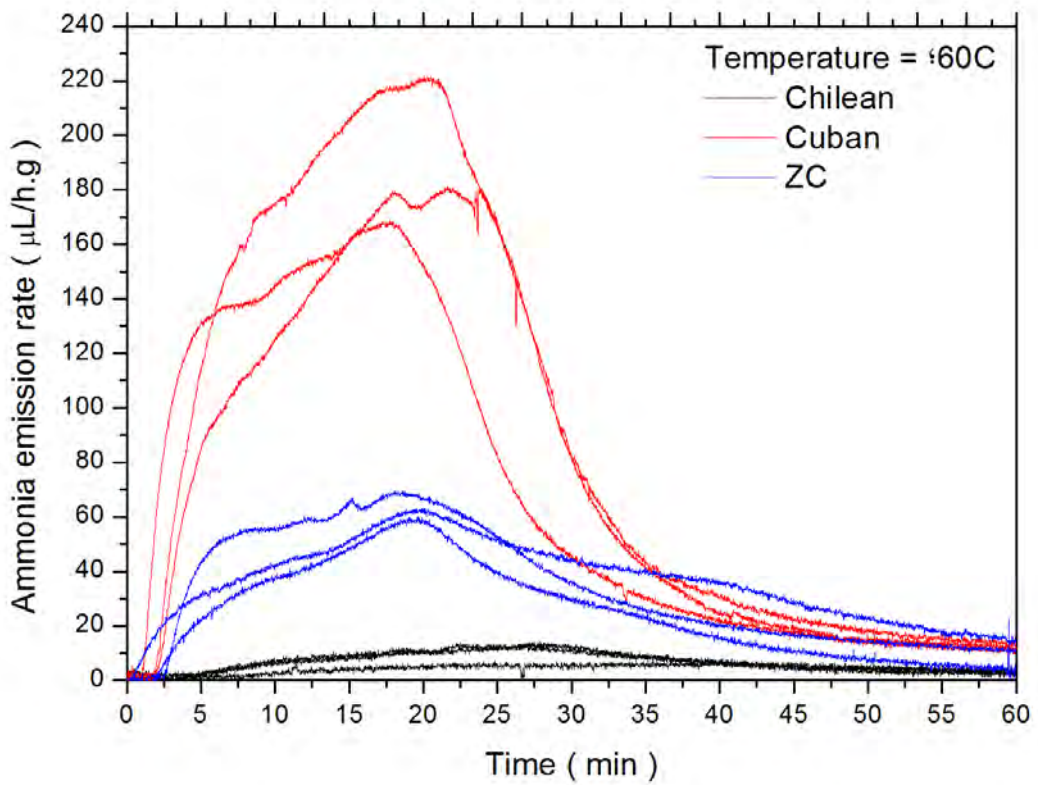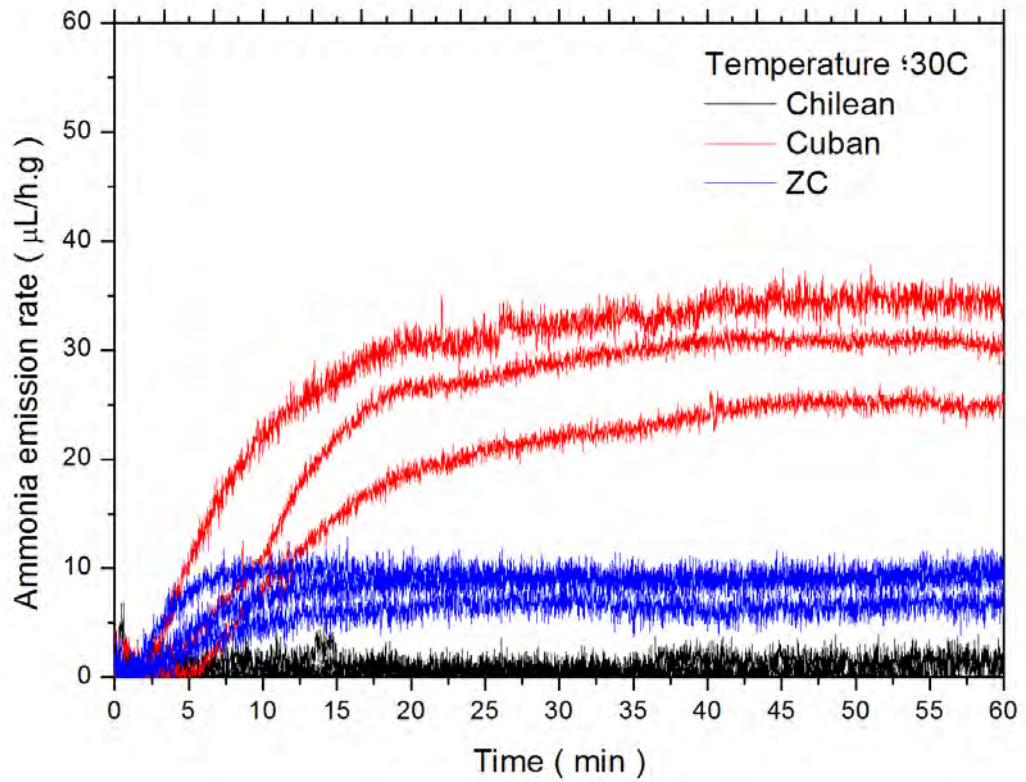
Figure 2.2: Ammonia emission rate from the materials treated with ammonium sulphate and monitored at 30°C(top) and $60^{o}C$(bottom).

Sample	N(mg) at 30^oC	N(mg) at 60^oC
Chilean	10.59	10.48
Cuban	10.02	11.08
ZC	4.88	3.96

Table 2.1: Nitrogen content in the materials determined by the Total Kjeldahl Nitrogen Method. The measurements were made with the same samples used in the ammonia emission monitored treated with ammonium sulphate (in both group of samples, 30^oC and 60^oC, respectively).

2.2.3   Conclusion

PAS have shown sensitivity enough to evaluate and compare the ammonia emission rate from the materials between three samples. Although Chilean zeolite has the highest specific area, it has shown smaller emission rate than Cuban zeolite. It can be justified because the higher acidity in the surface of Cuban zeolite that was found in the TPD measurements (data was not presented).The content of the zeolitic concentrate has between 40 and 60% of stilbite, the main content of Cuban zeolite, what makes the zeolitic concentrate, among the three studied zeolites, potentially available for application to improve the efficience of fertilizers on tropical soils. Finally, the ammonia volatilization rate from the different zeolites revelead they can be used for different proposals when applied to hold on the releasing of fertilizers.

2.3   Ammonia desorption in natural zeolites from 25^oC to 100^oC in rising ramp of temperature

This section presents the results found for measurements of ammonia emission rate for two natural zeolites (Cuban and National Zeolitic Concentrate - ZC). The samples were submitted to temperature sweep from 25 to 100^oC.

2.3.1   Material and Methods

Photoacoustic Spectroscopy based on Quantum cascade laser ($\lambda = 9.5\mu m$, P = 2 mW) was used for monitoring the ammonia emission rate from natural zeolites. The system used was the same described in the chapter 2 and in [3]. Two natural zeolite samples treated with an aqueous ammonium sulphate solution ($7.2\frac{g}{L}$) were submitted to a temperature ramp from 25 to

100^oC. A $10mL$ glass bottle with rubber lid was the sample holder. On the lid, two poliuretane tubes make the in- and outlet of carrier gas (pure nitrogen) flow, $5\frac{L}{h}$. The sample holder was placed on the thermoelectric element that makes the temperature sweep. A thermoelectric controller (Wavelength Electronics, LFI 3750) was applied and a computer program was written in Labview 7.0 (National Instruments) to produce the temperature ramp. A thermocouple from the thermoelectric control was placed in contact with the bottom of the glass surface, around $\frac{1}{4}$ of its height. Simultaneously to read temperature ramp, the software collected the photoacoustic signal acquired in the lock-in amplifier (Stanford Research Systems, SR850).

The samples ($1g$) were put in aqueous ammonium sulphate solution ($7.2\frac{g}{L}$) and stirred for three hours. Then, the material was filtered and $850mg$ of the solid material was placed in the bottom of the sample holder for ammonia emission monitoring. Initially, the temperature in the sample holder was remained at 25^oC. After 20 min at 25^oC of monitoring, a saturation of the ammonia emission was reached and the temperature sweep was began (rise rate = $0.05\frac{^oC}{s}$). Figure 2.3 shows the experimental setup used for the temperature sweep.
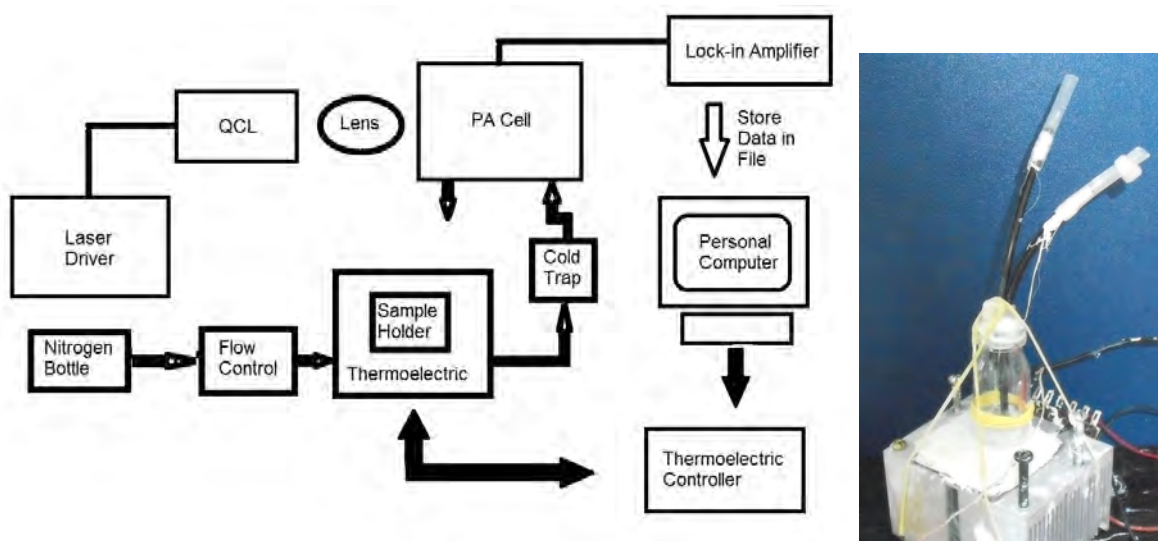
Figure 2.3: Experimental Setup (left) and sample holder on the thermoelectric (right). The glass is supported directly on the thermoeletric surface.

2.3.2   Results and Discussion

The measurements has began in the establishing of the temperature sweep. Heating tests for the sample holder were carried out by changing the temperature rate. Finally, we have decided for $0.05\frac{^oC}{s}$, because it was enough to heat the base of sample holder in low delay in the heating time. Figure 2.4 presents a example of reading and setting of the temperature

for the sample holder. We see reasonable concordance between the setting temperature in the themoelectric controller and reading temperature in the sample holder.
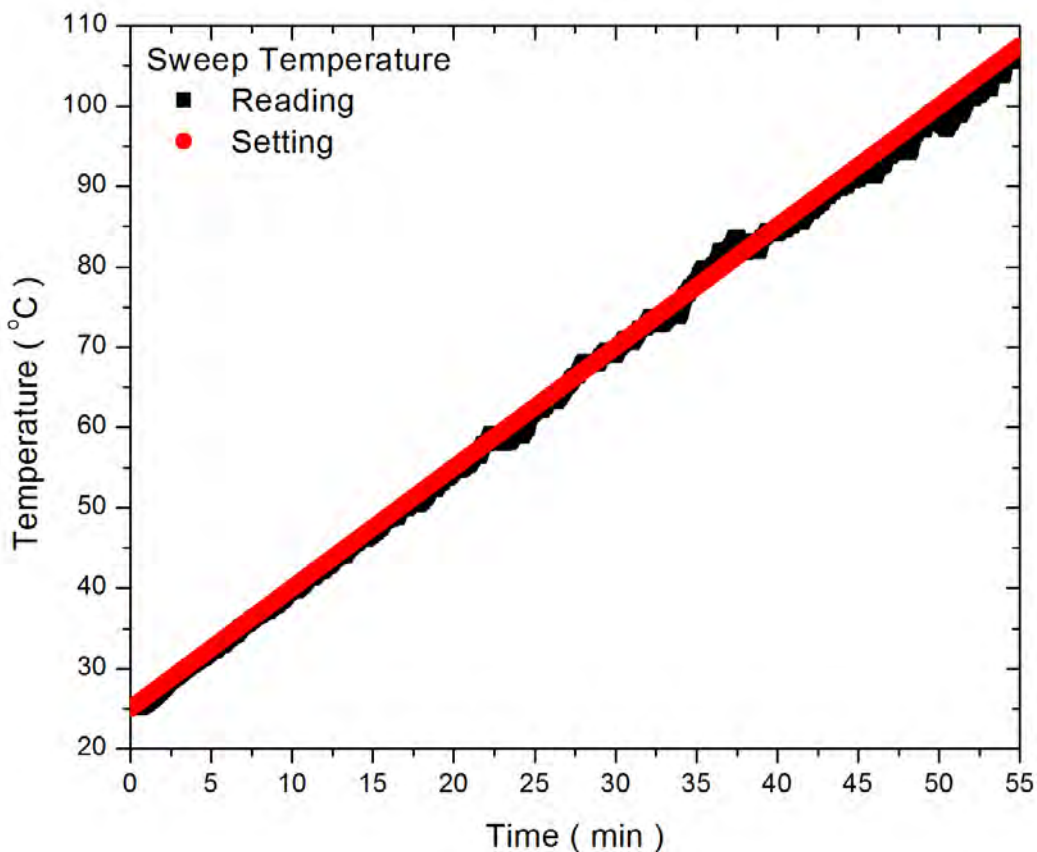
Figure 2.4: Temperature setting and reading during a temperature sweep.

After the preparation of the samples as described in the section 2.3.1, $850mg$ of sample was placed in the bottom (25^oC) of the sample holder and the ammonia emission rate monitoring has started. At the point where the ammonia emission rate has reached to be saturated was started the temperature sweep. Figure 2.5 are presented one measurement of photoacoustic signal versus temperature for ZC and cuban zeolite. Three repetitions were made for each sample, respectively.

The ammonia emission rate has reached maximum rate at 90^oC for both samples and started to decrease until the end of the sweep. Maximum ammonia emission rate for Cuban zeolite and ZC were, respectively, 460 and 65 $\frac{\mu L}{h}$. Integrating the ammonia emission curves, we determined that cuban zeolite and CZ have emitted $15.88 \pm 3.17mL$ and $1.67 \pm 0.36mL$ of ammonia, respectively. According to stechometry involved in the dissolution of ammonium sulphate in
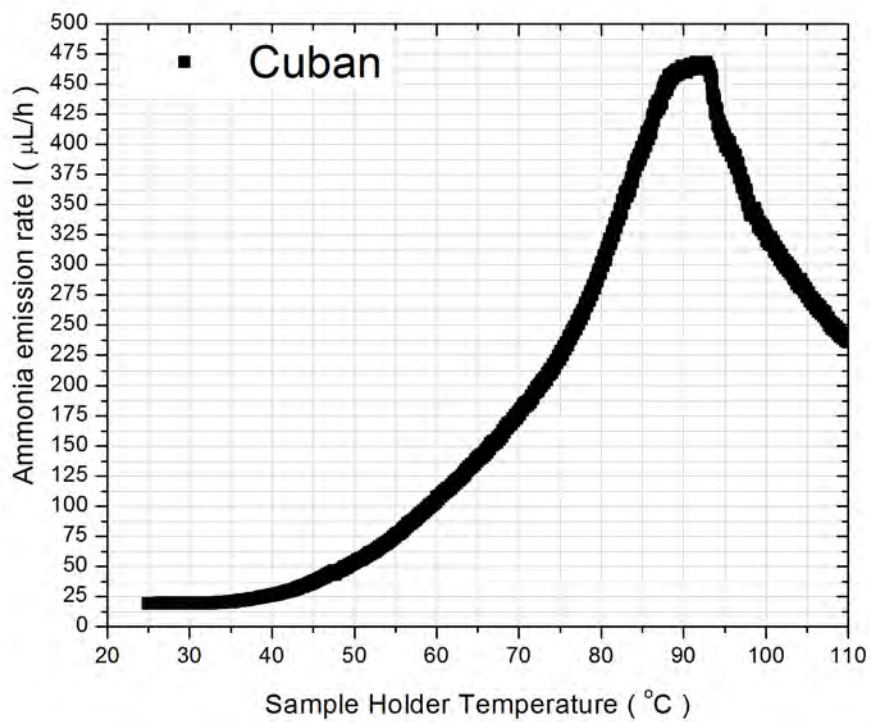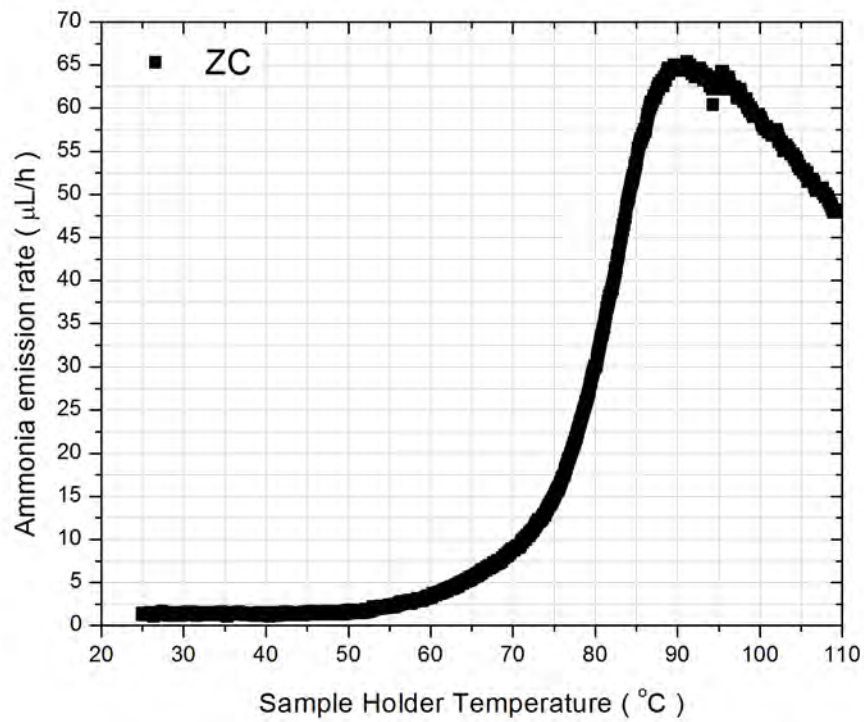
Figure 2.5: Photoacoustic signal as function of temperature for ZC (top) and Cuban zeolite (bottom) setting and reading during a temperature sweep.

water, ideally the full amount of ammonia available would be $122mL$ of ammonia (considering the full unbalance for ammonia instead of ammonium in $NH_4^+ \Leftrightarrow NH_3 + H^+$).

In range of temperature up to 100^oC, desorption is dominated by physical process. The break in the rising of ammonia emission rate at 90^oC could be related to the releasing of structural water physicaly adsorbed on the surface of the zeolite. On the other hand, the releasing of water could affect the equilibrium ammonium-ammonia, when we saw the decreasing in the ammonia emission rate. Typically, such amount of water in natural zeolites is an advantage for plant-soil system, because it can remain there for longer times to supply the soil and the plants with this water.

2.3.3 Conclusion

In this chapter, photoacoustic spectroscopy was used for monitoring the ammonia emission rate from natural zeolites treated with aqueous ammonium sulphate solution and, further submitted to a temperature sweep from 25 to 100^oC. The presented results were important for understanding the physical desorption of ammonia from such materials. These materials are promised for improving the efficiency of fertilizers in tropical soils. Typically, such soils can reach to temperature as high as 60^oC. On the other hand, the shock of the first hours after spreading of fertilizer on the soil could be critical for the lifetime of fertilizer, specially, because humidity and temperature.

The results found for the temperature ramp revealed a critical point for ammonia desorption at 90^oC, which could be related to the releasing of water. This evidence can be funded, if we look to the unbalance ammonium-ammonia. The presence of water can influence on the pH of the surface, then on the equilibrium of ammonium-ammonia. Another important aspect is the amount of ammonia release after the temperature ramp. In the same sense of the results found the section 2.2, the cuban zeolite has presented higher amount of ammonia emitter than ZC in comparison. That fact makes more clear the real potential of the cuban zeolite to retain ammonium. Also, it is clear the potential ZC to retain ammonium, even in a lower level in comparison with the cuban zeolite. Finally, the results found in this chapter are important for future projects, where such system could be improved as the system would be able to do an ammonia temperature desorption programmed up to 500^oC.

Chapter 3

Application of DFB diode laser $(\lambda = 1531.51\eta m)$ for ammonia traces detection in two differential PA cell

3.1 Introduction

In this study, the performance of a Differential PA cell and a Small version of a Differential PA cell (figure 3.1) for trace gas detection were compared. As source of radiation for ammonia detection, a diode laser was employed. The laser radiation was collimated into each photoacoustic cell using fiber collimator. Spectrometers based on diode laser are interesting because of the easiness of operation and high level of available power for some models. Especially for ammonia, diode lasers emitting around $1531\eta m$ have low water and carbon dioxide absorption [6], resulting in a photoacoustic signal free from interference of such air molecules. This fact calls attention for the use of such system to study biological and agricultural systems. Also, for sensors that are intending to be used more close to the Green houses and properly to the field, it looks better to have lighter and more robust cells. Diode lasers combined with a fiber-coupled diode lasers have also advantage for alignment on time. The alignment for both cells was simplified by the use of the collimator attached at the body of each cell.

The performance of differential PA cells was already exhaustively tested previously [36, 37, 45] and some applications are presented in the literatures for ammonia trace gas detection [3, 4, 38]. Although the differential PA cell has already a good performance, the new concept of a small differential cell combined with fiber-coupled diode laser meets the desired criteria for size,

weight, ruggedness and portability that is required for agricultural application. The compact cell is a half dimensions version of differential PA cell with acoustic resonance centered around $7000Hz$.
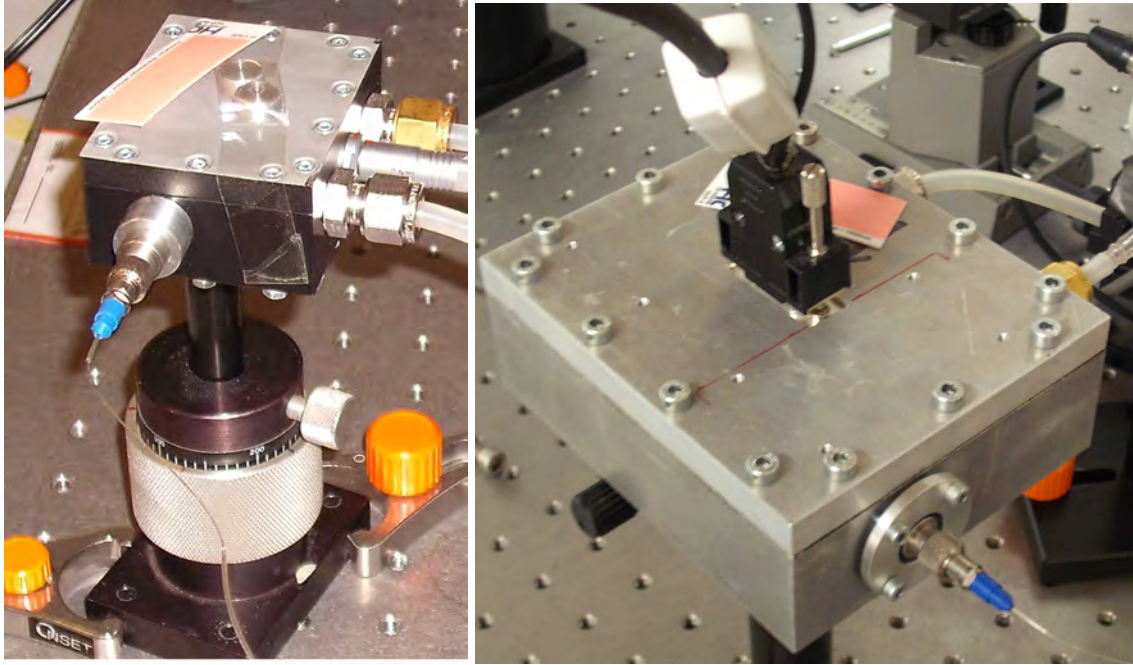
Figure 3.1: Small Differential PA cell (Left) and Traditional Differential PA cell (right).

A diode laser emitting at $1531.51\eta m$ was used to excite the ammonia molecules. The ammonia absorption in that wavelength is interesting because of the low absorption of water and carbon dioxide [5]. Furthermore, many articles have reported ammonia detection in that wavelength range recently [1, 6, 13]. In this work, in order to evaluate the performance of the photoacoustic spectrometers, the photoacoustic signal generated due to absorption process in a mixture of $50ppmV$ of ammonia in nitrogen was monitored and compared with the background signal produced when the photoacoustic cell is submitted to constant flow of pure nitrogen.

3.2   Methodology

The performance of the photoacoustic cell was determined by comparing the photoacoustic signal obtained for certified mixture of ammonia 50 ppm diluted in nitrogen with the background signal characterized by nitrogen. The flow for both cells was kept constant at $300sccm$ by mass flow controllers (Tylan model FC260). A DFB fiber coupled diode laser emitting at $1531.51\eta m$ (EM4, Model AA1401-195600-080-PM250-FCA, Output Power $100mW$; diode controller Melles Griot 06DLD103) attached in fiber collimator (Thorlabs, FC230FC-

$1550\eta m$, anti-reflection coating $1050 - 1620\eta m$ - Figure 3.2) was used as radiation source. The main absorption coefficient for ammonia in the range of that laser is around $1531.51\eta m$ ($\alpha = 14 \times 10^{-6}cm^{-1}$ for 50 ppmV, Reference: Northwest Infrared Database). The diode laser current was modulated by a sinus waveform from an internal reference of a Lock-in amplifier (Stanford Research Systems, SR850, Sample rate $1Hz$) in wavelength modulation and amplitude modulation (WM-AM).
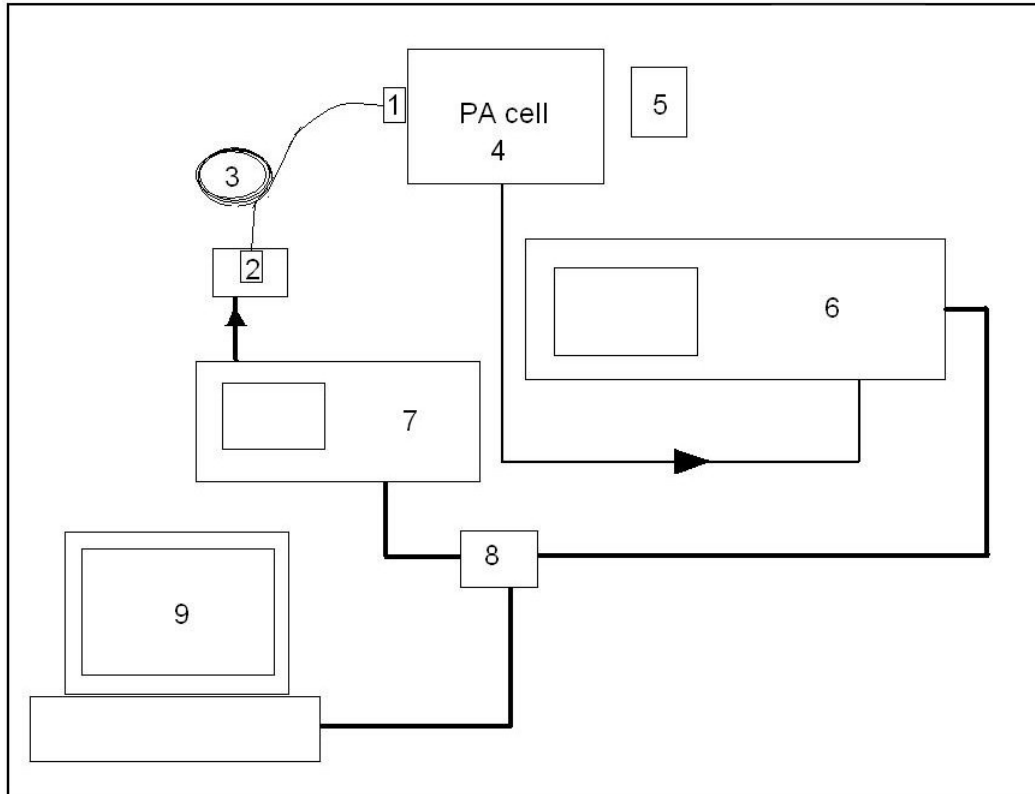
Figure 3.2: Experimental setup: 1.Fiber Collimator, 2. DFB diode laser and housing, 3. Fiber optic, 4. PA cell, 5. Output power meter, 6. Lock-in amplifier, 7. Diode Laser controller, 8. GPIB interface and 9. Personal Computer.

The current in the laser was fixed at $420mA$ and an increment of $11mA$ was overlapped to the base current in the time by employing a sinus waveform voltage. In order to tunning the wavelength emission, the temperature of the laser was changed during the measurement. It was changed at $0.03\frac{^oC}{s}$. A program made in Labview and based on the GPIB (National Instruments, GPIB controller for Hi-Speed USB) was used to interface the diode laser controller and the lock-in amplifier through to a personal computer. The reading of temperature from the diode laser, current and PA signal were stored in a text file. The PA signal generated by the standard photoacoustic cell was four times pre-amplified before to feed the lock-in

amplifier. The PA signal from the small photoacoustic cell was directly amplified by the lock-in. The Differential cell and the smaller version of the Differential PA cell are equipped with electrets microphones (Knowles Electronics, EK-23024-000, Sensitivity $28\frac{mV}{Pa}$ and TM-24547-C36, Sensitivity $20\frac{mV}{Pa}$, respectively).

In the emission range of each diode laser, the wavelength that meets the highest absorption peak for ammonia was located by a temperature scan of the diode laser. After that, the wavelength for the highest absorption peak was set keeping the temperature of DFB the diode laser constant. The PA signal respective to the absorption spectrum for ammonia and monitoring at fixed temperature in the diode laser was acquired for each cell. By the contrast between the highest absorption coefficient for ammonia $50ppm$ and background , the minimum absorption coefficient was determined and the lower limit detection of each cell was established. The setup constant was defined by [36, 33, 42]:

$$C = S_{PA-NH_350ppm}/S_m.P.\alpha_{NH_350ppm} \tag{3.1}$$

S_{PA-NH_350ppm} is the PA signal for ammonia 50 ppm diluted in nitrogen as α_{NH_350ppm} is the absorption coefficient for ammonia $50ppm$. S_m is the sensitivity of the microphone and P, the output power of the Laser. Based on such parameter and the lowest measured PA signal (S_{Min-PA}), $S_{Min-PA} = S_{background} + \sigma_{Background}$, where $S_{background}$ is the background signal and σ_{NH_350ppm} is the standard deviation for the PA signal for ammonia $50ppm$, we have defined the minimum absorption coefficient for ammonia from lowest limit of concentration for the system:

$$\alpha_{min} = S_{min-PA}/C.P \tag{3.2}$$

3.3 Results and Discussion

The PA signal for two differential PA cells was evaluated using ammonia as test gas. The performance of the differential PA cell was already reported previously for ammonia trace monitoring and detection [36, 37]. The temperature scan was carried out for the differential PA cell from 15^oC to 21^oC. For the small differential PA cell, the scan was made from 12.5^oC to 18.5^oC. The figure 3.3 pick out the amplitude of PA signal and its X and Y components were acquired during the course of the temperature scans. The temperature corresponding to the main absorption line in the temperature scan was chosen for each cell.
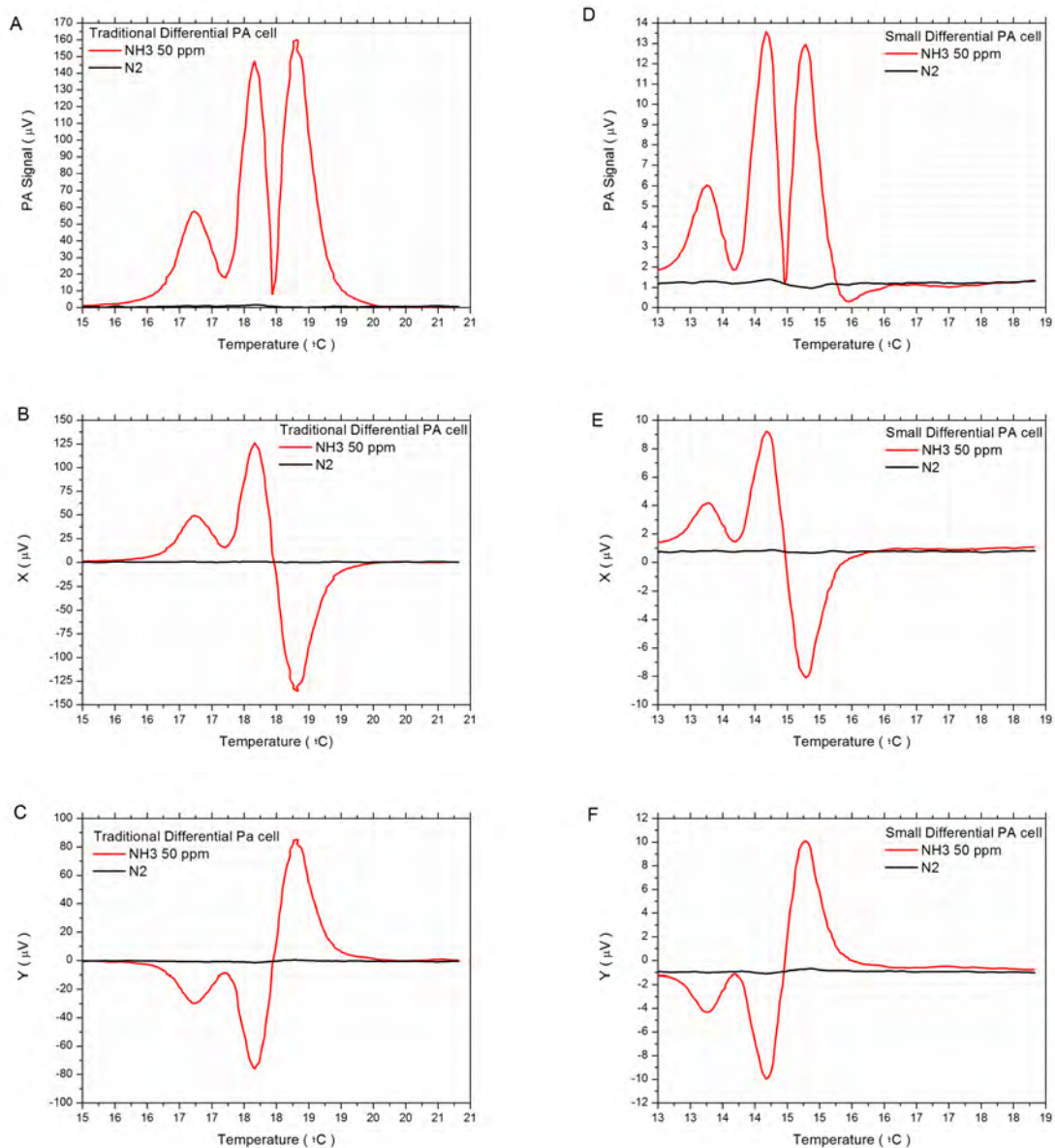
Figure 3.3: PA amplitude signal and its X and Y components for ammonia 50 ppm absorption spectrum and background for the two PA cells are presented.

Further, the PA signal in amplitude was monitored on the time and the change from ammonia $50ppm$ to nitrogen in the gas line was accomplished. For the small differential PA cell, the highest photoacoustic amplitude signal for 50 ppm of NH_3 in nitrogen was obtained when the temperatures of the laser were set at 18.3^oC (PA signal = $160\mu V$) and 14.0^oC (PA signal = $13.5\mu V$), as shown respectively in figure 3.3.A and D. The PA signals were acquired for minimum 10 minutes for each gases. Based on these monitoring of PA signal (see figure 3.4), we have made the calculations for the minimum absorption coefficient for ammonia, low limit detection and sensitivity of each system. The results found and determined lay in the table 3.1.

PA Cell	Resonance Frequency	Q_{Factor}	$S_{NH_3 50ppm}(\mu V)$	$\sigma_{NH_3 50ppm}$
Traditional	3860.22Hz	17.34	1.78×10^{-4}	5.19×10^{-7}
Smaller	6429.36Hz	13.45	1.59×10^{-5}	3.39×10^{-8}
PA Cell	$S_{Background}(\mu V)$	$\sigma_{Background}$	$\alpha_{min}\ (cm^{-1})$	
Traditional	2.00×10^{-6}	1.46×10^{-7}	5.36×10^{-9}	
Smaller	1.41×10^{-6}	2.60×10^{-8}	2.60×10^{-8}	
PA Cell	c_{min}	σ_{min}	$D_{PA}\ (cm^{-1}.W)$	
Traditional	6.85×10^{-7}	4.10×10^{-8}	5.36×10^{-10}	
Smaller	4.68×10^{-6}	8.18×10^{-8}	2.60×10^{-9}	

Table 3.1: Parameters determined based on the PA signal for ammonia and background for the cells.

The Q[1] factor of 17 for the differential PA cell was found that is in good agreement with what was reported in the past [36]. The standard deviation for the ammonia and background signal were found as 519 and 146 ηVolts , and 33.9 and 26 ηVolts, respectively for differential cell and small differential PA cell. Based on the equation 1.5 , we have determined the lowest limit detection of $700 ppbV$ for the differential PA cell and $4.5 ppmV$ for the small differential PA cell. In the same way, the minimal variations in the concentration were found as $40 ppbV$ and $80 ppb$, respectively. Comparing these results with others found in the literature for diode lasers, they are much better for the differential PA cell in this case.

The microphone of the small differential PA cell probably has a strong limit of sensitivity in the range of the used resonance frequency. In spite of such limitation, its dimension and weight compose many advantages for some applications. In general, the lowest limit detection that was found for the small differential PA cell is already interesting for some applications, which demand more mobility of the setup for transportation and easy installation around the measurement field, quasi *in loco* measurement.

3.4   Conclusion

The performance of two PA cell was investigated. One of them was already tested previously and its importance to this study was due to the fact of it to be a good reference for

---

[1]$Q = \frac{f_o}{\Delta f}$. f_o is the center frequency and Δf is the Full Width at Half Maximum (FWHM).

comparison. The performance of the small differential cell was not sensitive like the differential PA cell, but it has already some advantages which could be explored for some applications. The use of diode laser with output power as high as $100mW$ provided good sensitivity for differential PA cell.
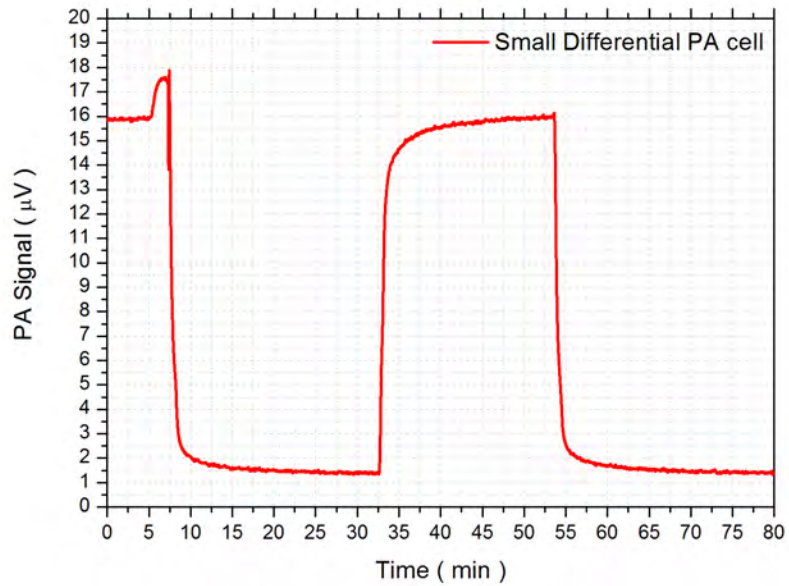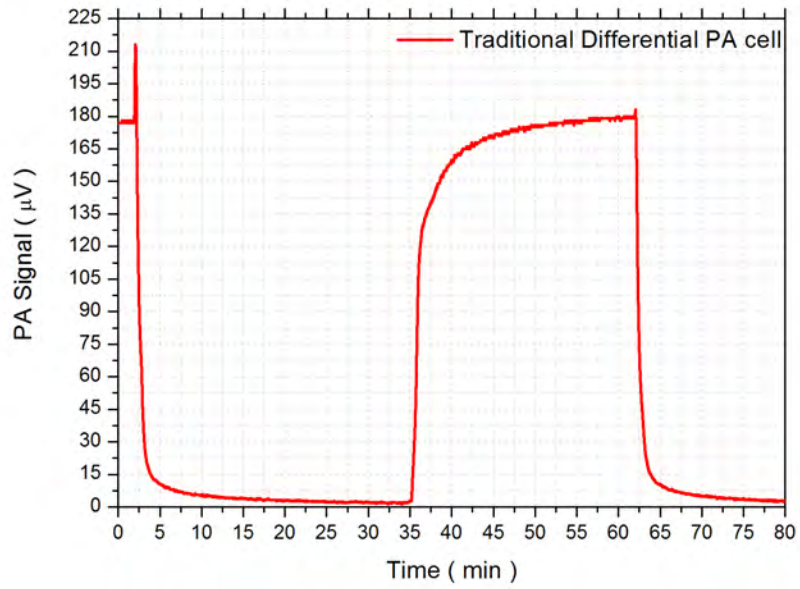
Figure 3.4: PA signal for the change from ammonia 50 ppm to background at fixed temperature for each PA cell.

Chapter 4

Implementation of a Software-Based lock-in (SBLI) and its application for simultaneous detection of nitric and nitrous oxide trace gas with Photoacoustic Spectroscopy

4.1   Introduction

Lock-in amplifier is an essential device for a photoacoustic spectroscopy experimental setup. It works as a phase-sensitive signal detector, acting like a very selective and narrow band pass filter, centered at modulation frequency of the radiation or excitation source. A lock-in amplifier has the ability to extract very low intensity AC signal, even when it is completely buried in noise, giving also the signal phase information. A conventional lock-in amplifier is a high cost analytical laboratory device, which has additional functions such as signal filtering and data acquisition module. The dimensions of a typical lock-in amplifier can limit the compatibility for a compact experimental setup. Furthermore, such devices are normally not capable to execute non-conventional photoacoustic signal processing. In the last ten years, the use of data acquisition (DAQ) cards has become quite popular for applications that involve automation and control of homemade measurement systems in laboratory. Some of such cards combine low cost, good performance and multiple access possibilities (analog input and out-

put, digital I/O ports and counters). Examples of proposals that implement softwares based on lock-in algorithim using DAQ cards can be found in [1, 7, 12, 15, 19, 20, 43] and some are even commercialized. In this sense, Labview is a graphical programming language based on virtual instrument concept, which simplifies data acquisition procedures, hardware interfacing and remote control of instruments. Simple task can be build to acquire data from DAQ cards and process signal with simple tools.

In diode-laser based photoacoustic spectroscopy (PAS), a high selectivity diode laser is used to excite roto-vibrational modes in individual and exclusive molecules. For the multi-molecules trace detection using an unique sensor, the system demands different diode lasers emitting at specific absorption wavelength range for each chemical specie. For such propose, it would be also require multiple lock-in amplifier detection, due to the necessity of modulating individually each diode laser at different frequencies. Such scheme for wavelength modulation spectroscopy [22] was already proposed. For a proposal involving two diode lasers, we would need three lock-in amplifiers for the complete demodulation of the PA signal. This is a complex experimental scheme, demanding space, multiple instruments interfacing, besides the processing time and costs involved. In this way, the use of DAQ cards for digitalizing the PA signal and software-based lock-in detection looks quite interesting. Recently, different works have already shown the viability of using based lock-in detection on DAQ cards [7, 19, 43]. A unique DAQ card can digitalize, process the PA signal lock-in operation and simultaneously modulate multi-diode lasers at different frequencies.

In this work, we have proposed the development of a Labview routine using a DAQ card (National Instruments, M Series, PCI 6281 and NI USB 6216) for development of a synchronous system, with phase-sensitive detection. As first step, a diode laser was modulated for ammonia trace detection using a photoacoustic differential cell. The PA signal was extracted using a conventional lock-in amplifier as well as using the software-based lock-in and DAQ card. As second step, a DAQ card was applied to modulate two quantum cascade laser at different frequencies. The two laser beams were aligned through a PA cell and the resulting PA signal was demodulated by a computer program in Labview.

4.2 Materials and Methods

4.2.1 Comparing the performance of a software-based lock-in detector and DAQ card with a conventional lock-in amplifier.

A routine in Labview (version 7.1, National Instruments) was developed to perform as a lock-in detector. An analog output from a DAQ card (PCI NI 6281) was used to synthesize a sine waveform to modulate the current of a diode laser, while the analog signal from the differential PA cell was used as input signal and digitalized by the card [36]. The PA cell used to detect ammonia has a resonance frequency of $3822Hz$. As radiation source a DFB diode laser - figure 4.1 - ($\lambda = 1531.51$nm, EM4, Model AA1401-195600-080-PM250-FCA, Output Power $100mW$; diode controller Melles Griot 06DLD103), was employed. The temperature of the laser was fixed at 23^oC that corresponds to a peak of power of about 100 mW centered at $1531.51\eta m$. Figure 4.2 shows a spectrum of 50 ppm of ammonia in nitrogen. Thus for the wavelength of $1531.68\eta m$, it is expected absorption coefficient of about $14 \times 10^{-6}cm^{-1}$. The same synthesized sine waveform used to modulate the diode laser was reference signal for the lock-in. The laser current was then modulated in both amplitude and wavelength modes. For comparison purpose, the PA signal was also received and extracted by a conventional lock-in amplifier (Stanford Research Systems, SR850), connected to a PC using a GPIB interface.
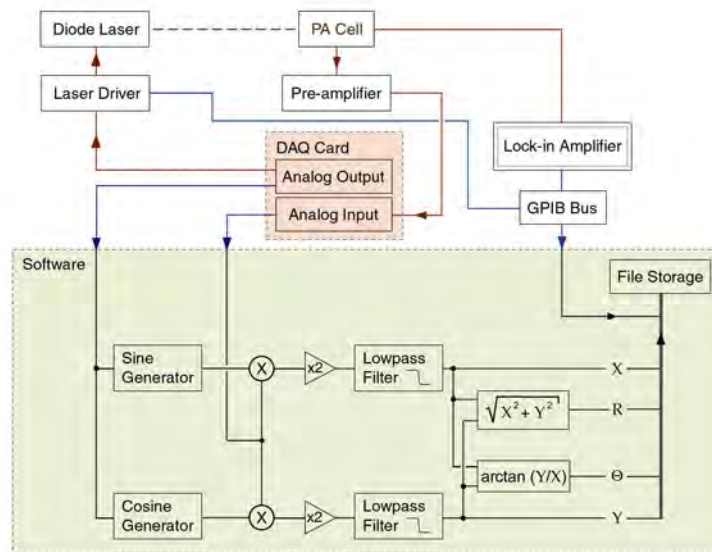

Figure 4.1: Scheme based for the software-based lock-in, including the experimental setup, DAQ card and pre-amplifier.

The DAQ card input (A/D) and output (D/A) channels were set to operate in continuous mode, using the available internal hardware data buffers. The data acquisition and generation were synchronized by using the same sampling rate (200kSamples per second). First, PA signal was acquired by a conventional lock-in amplifier and then by a DAQ card, follow by a signal processing routine that implements the lock-in operation. The routine had its frequency and phase on time registered and from that information, a pure sine and cosine waveforms were individually generated and introduced to the routine that performs the lock-in in-phase and quadrature operations. Both sine and cosine waveforms were generated with the same sampling rate and number of samples as set to the input and output channels of the DAQ card. The resulting PA signal was individually multiplied by these both reference signals and processed by a low pass filter and finally stored in files, together with the data collected from the conventional lock-in.
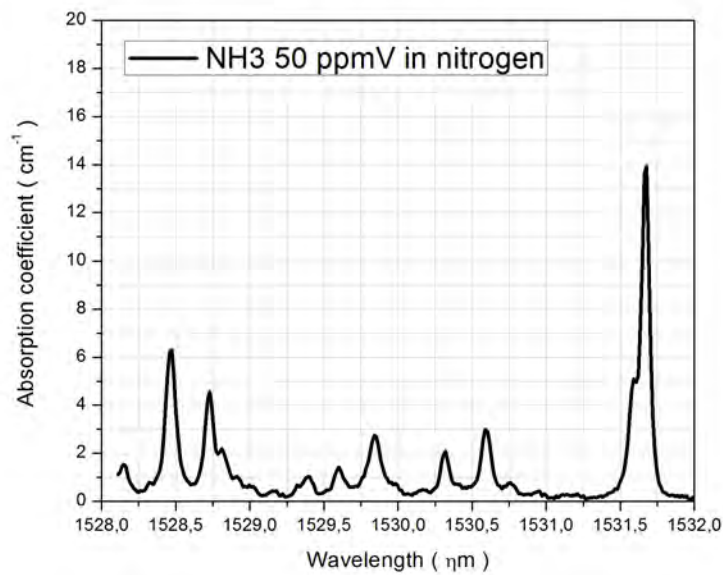
Figure 4.2: Absorption coefficients for ammonia 50 ppmV in nitrogen between 1529 and 1532 nm. Source: Northwest Infrared Database.

The time constant for the virtual lock-in was defined as three times the inverse of cutoff frequency for lowpass filter, in order to compare the performance of both systems in similar operation conditions. At the end of the program algorithm, the PA signal and its components (in-phase and quadrature components, magnitude and phase information[1]) were stored in a file

---

[1]Amplitude R comes from the relation $\sqrt{X^2 + Y^2}$ and phase, ϕ, comes from $\frac{360}{2\pi} \times \arctan \frac{Y}{X}$. R is called amplitude, X is in-phase component and Y, quadrature component.

for the software-based and the conventional lock-in, as well as diode laser temperature and other auxiliary experimental data.

4.2.2 Dual Laser simultaneous modulation for Nitric oxide (NO) and Nitrous oxide (N_2O) trace detection

For the dual laser simultaneous detection, the Labview routine made for mathematic lock-in operation, described in section 4.2.1, was duplicated in the software. It was adapted for another DAQ card (National Instruments, M Series, NI USB 6216) for running two lock-in devices simultaneously. This card has two digital to analog output channels (set in the range from $-6V$ to $6V$), which makes it able to generate two independent output signals at different frequencies and amplitudes. An analog to digital channel input set for the range from $-300mV$ to $300mV$ was used to receive the pre-amplified PA signal. The sampling rate of analog input and output was made continuously at 200 kilo samples per second. The QCLs (model SB745DN, $\lambda = 7.7\mu m$, P = 2 mW and model SBCW1534DN for nitrous oxide, $\lambda = 5.27\mu m$, P = 20 mW for nitric oxide absorption excitation) were modulated using amplitude modulation mode. Their beams were aligned so that their waists are at the center of the resonant tube in the PA cell. Each laser was put in front of the windows of the cell (figure 4.3 and figure 4.4). The temperature of the diodes were set in order to sweep same ranges of temperature (from -15 to 15^oC), where there are absorption lines for nitrous oxide and nitric oxide (Figure 4.5).

The center of resonance profile in the PA cell is at 3850 Hz (FWHM = 200 Hz, typical Q factor around 18) for the mixture of N_2O 2.5 ppmV in nitrogen and NO 2.5 ppmV in nitrogen (full flow = 100 sccm). The lasers modulation frequencies were chosen to stay 20 Hz off the acoustic resonance of the cell (3830 Hz for one laser and 3870 for the second one). By using this new procedure, we eliminate the need to use three frequencies for such dual diode laser modulation, as proposed in previous works [22], namely cascading lock-in demodulation. Additionally, the choice for values of frequencies close to the resonance frequency of the PA cell avoids the use of long time constants in the lock-in filtering stage and thus more integration time. The generated data were stored in a file for analysis and comparison.

Three different procedures of detection were tested: 1) The absorption spectrum of each molecule was collected turning the wavelength by changing the temperature of the lasers from -15^oC to 15^oC. During the simultaneous measurements of N_2O and NO the flows of the gases were fixed at 50 sccm; 2) Identifying the absorption peaks for N_2O and NO by the wavelength
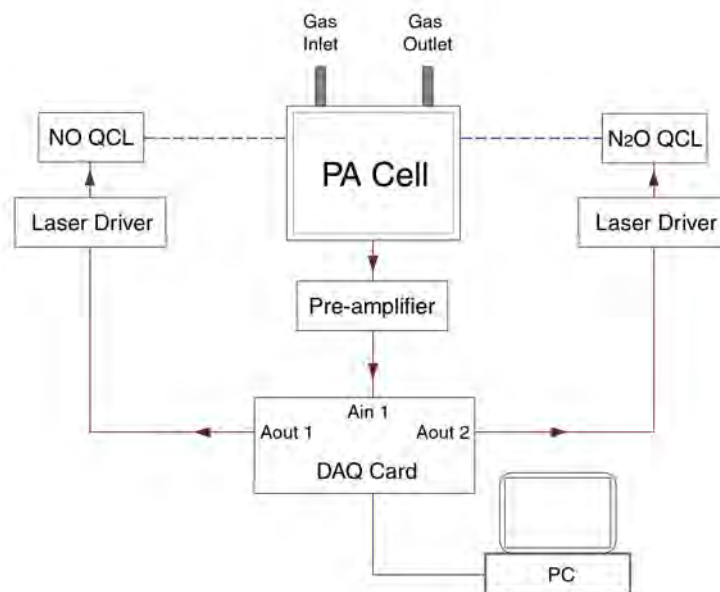
Figure 4.3: Experimental Setup mounted for two QCLs in the same PA cell. The PA signal from the electret microphones was amplified to the milivolts range using a differential low noise homemade pre-amplifier. In the following, this amplified signal was digitalized in the DAQ card.

scans, the temperature of each diode was set to the corresponding maximum absorption line of each molecule (-6.6^oC for N_2O and -10^oC for NO) and the resulting PA signals were collected as function of the time. After 10 minutes of detection, the flow was changed to a flow of pure nitrogen (100 sccm) for 10 minutes followed again by the mixture of N_2O and NO. The PA signal measured when the PA cell was purged by nitrogen was used as background signal; 3) The PA signal was registered changing consecutively the flow (100 sccm) among nitrogen, nitrous oxide and nitric oxide.

Figure 4.4: Laboratory workbench. A and B are QCLs. C is the PA cell.

Figure 4.5: Absorption spectra for N_2O and NO (reference for 5 ppmV in nitrogen) at different emission wavelengths for the two diode lasers. Source: Northwest Infrared Database.

4.3 Results and Discussion

4.3.1 Software-based lock-in using DAQ card: PAS setup based on DFB diode laser for ammonia trace gas detection

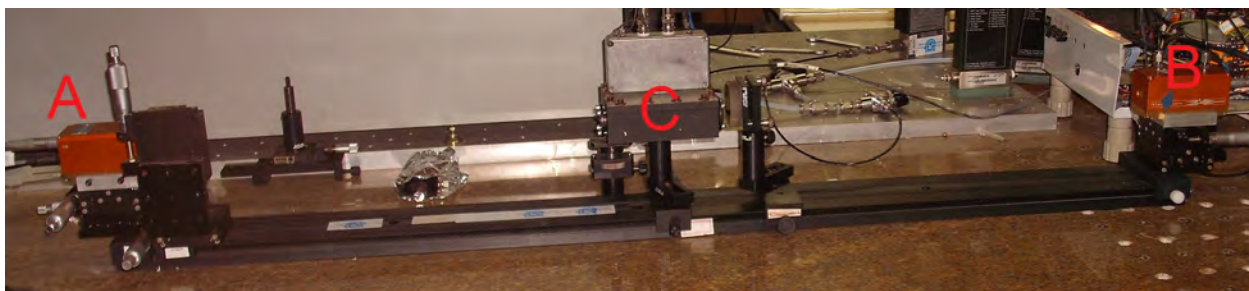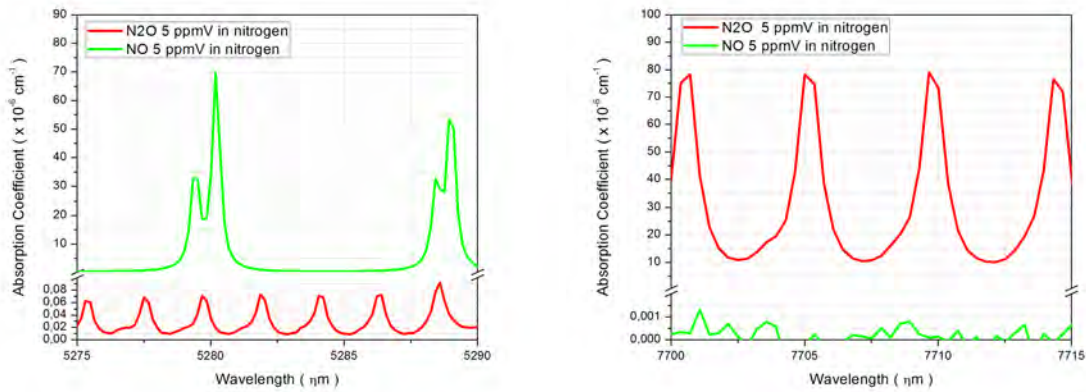An experimental setup for ammonia trace gas detection was mounted for testing the performance of the virtual lock-in by comparing with a conventional lock-in amplifier. By using a GPIB interface, a Labview made routine was responsible for sweeping the temperature in the diode laser and thus changing its wavelength. The same program ran the lock-in detection processing. The photoacoustic signal due to the absorption of ammonia was collected by the conventional lock-in amplifier and stored. The time constant of one second was used. This value corresponds to three times the inverse of the cut-off frequency of a low-pass filter, implemented in software.

The first test was to check the synchronism and quality of the analog output waveform generation. This is essential to have a properly modulated laser current and supply a good reference to the conventional lock-in amplifier. Noise based on loose of synchronism and random changes in the phase of the signal can be a critical problem in such system. Even in a conventional lock-in amplifier, which has phase-looked loop (PLL) system, it could be a disturbance for the lock-in operation, in spite of such PLL system normally correct the phase differences between the signal and reference. A software generated sine waveform was set to produce 5 V peak-to-peak amplitude. The sine waveform generated through the analog output was 3822.1 Hz showing a standard deviation of 0.3 Hz. We have begun the measurement checking the difference on the

47

PA signal when the laser is ON and OFF (OFF - broken the incident light; Figure 4.6), when the PA cell was filled with nitrogen.

First setting the laser wavelength to the corresponding highest absorption line ($\lambda = 1531.68\eta m$), we have begun the analysis checking the difference in the PA signal when the laser was ON and OFF. Figure 4.6.A, B, C and D show the magnitude of the PA signal R, its in-phase component X, quadrature component Y and, Phase, respectively. The fact that the value of R obtained for the virtual lock-in was one order bigger than that obtained for SR850 lock-in is not relevant because it is just an electronic amplification factor of 10. On the other hand, X and Y components show interesting behavior since their values are related to the difference of phase between the absorption process and the processing PA signal. Figure 4.6.D shows the phase of the PA signal, again red color corresponds to software-based lock-in amplifier, and black to the SR850. The value of $\Delta\phi$ obtained for the virtual ($\Delta\phi_{SBLI} = 1.9^o$) was smaller than that obtained for the SR850 ($\Delta\phi_{SR850} = -29^o$). Such result reflects the effect of the time constant on the processing PA signal that decreases as the value of $\Delta\phi$ decreases. The higher value of standard deviation for the PA signal components (R, X and Y) obtained by the virtual lock-in corroborate to the difference for the time constant. The results show good agreement between the magnitudes of the signal obtained for both lock-ins.

In the sequence, figures 4.7.A and 4.7.B present results for amplitude of PA signal for ammonia 50 ppm in nitrogen absorption and the background signal for the same modulation condition, respectively. Diode laser was modulated in amplitude. The current was set as 225 mA and a sinus waveform with 225 mA of amplitude and frequency equal resonance frequency of the PA cell made such current changes in the time.

Again it was possible to state a good agreement between both lock-ins. A remarkable characteristic is the resolution of spectra obtained by using the Software-Based lock-in. A spectral structure located on left side of the main absorption peak (indicated by an arrow) was better resolved by the Software-Based lock-in. It is again an intrinsic characteristic when small time constant is applied. By purging the photoacoustic cell with nitrogen, as expected, the PA signal returns to the background signal (Figure 4.7).
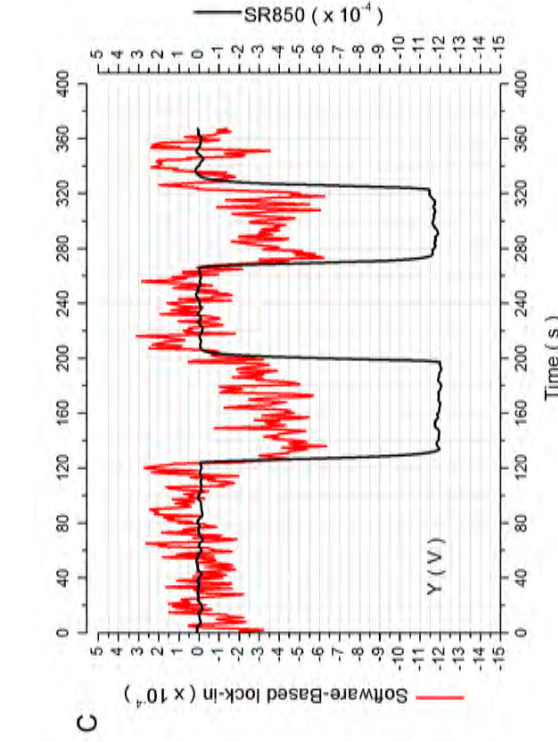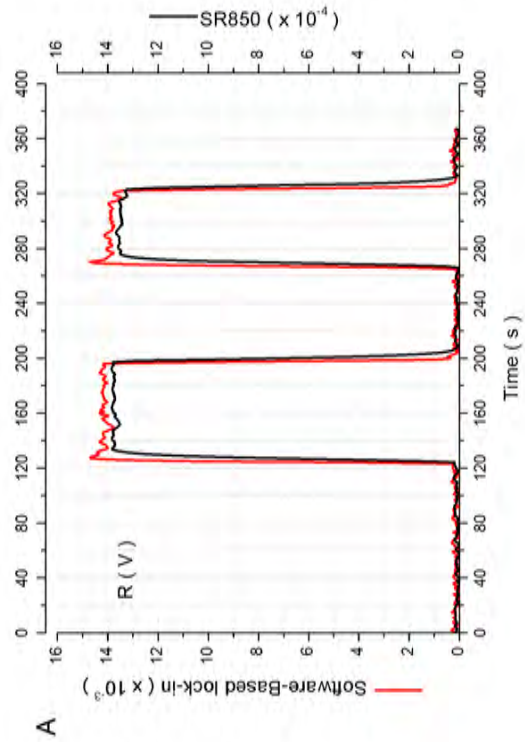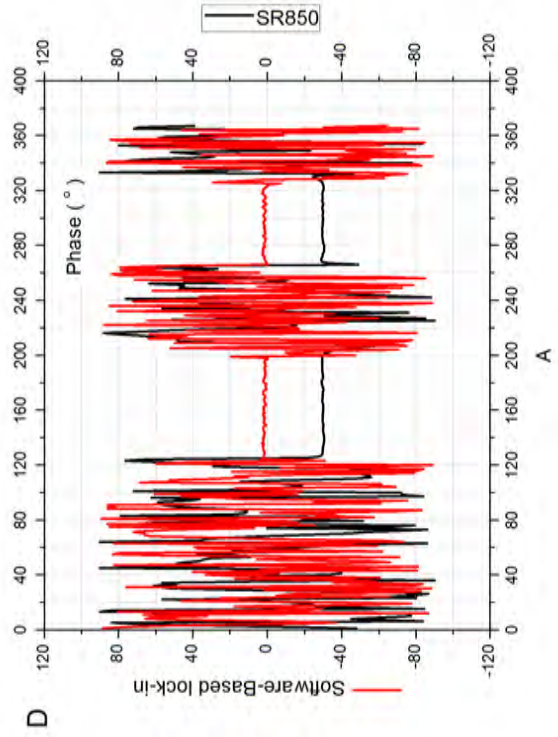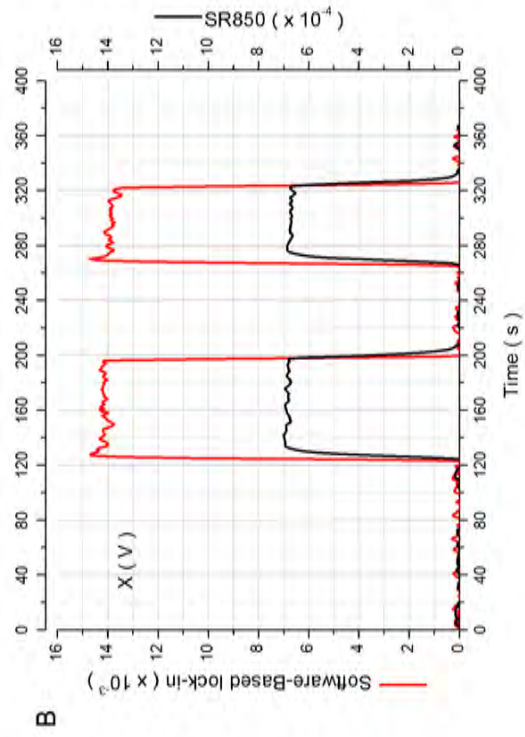
Figure 4.6: First test for the system DAQ card and conventional lock-in amplifier. The result for the PA signal when the state of the laser was changed from OFF to ON.

49
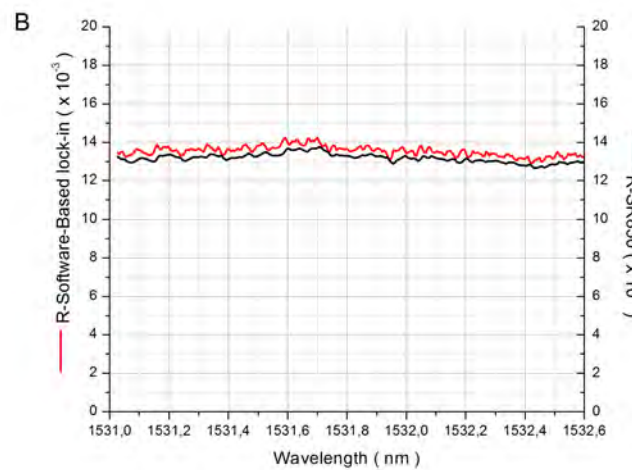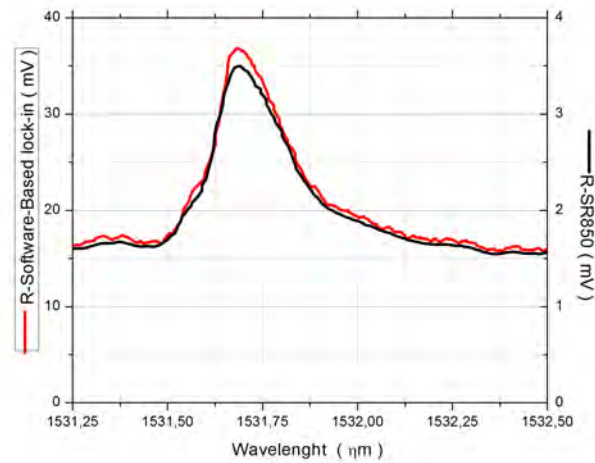
Figure 4.7: In graph 4.7.A is amplitude of the PA signal produced by absorption of ammonia standard sample 50 ppm in nitrogen. Graph 4.7.B is PA signal for nitrogen (background signal) in the same range of wavelength. Diode laser was modulated in amplitude. The current was set as 225 mA and a sinus waveform with 225 mA of amplitude and frequency equal to resonance frequency of the PA cell made such current changes in the time.

The samples were changed from nitrogen to ammonia 50 ppm (Figure 4.8.A and 4.8.B). We see clearly that the DAQ card acquisition and the software signal processing were fast enough to detect changes in the PA signal, similar to those data obtained by the conventional lock-in amplifier, showing no lose of information. The measurements shown in Figure 4.8.A was made using 1 s of time constant in the software-based lock-in and the time constant of the conventional lock-in was kept at 1 s. Figure 4.8.B was made based on 300 ms time constant for both lock-ins. Actually, it was very difficult to synchronize the data acquisition of both systems, mainly due to GPIB interface access times.

50
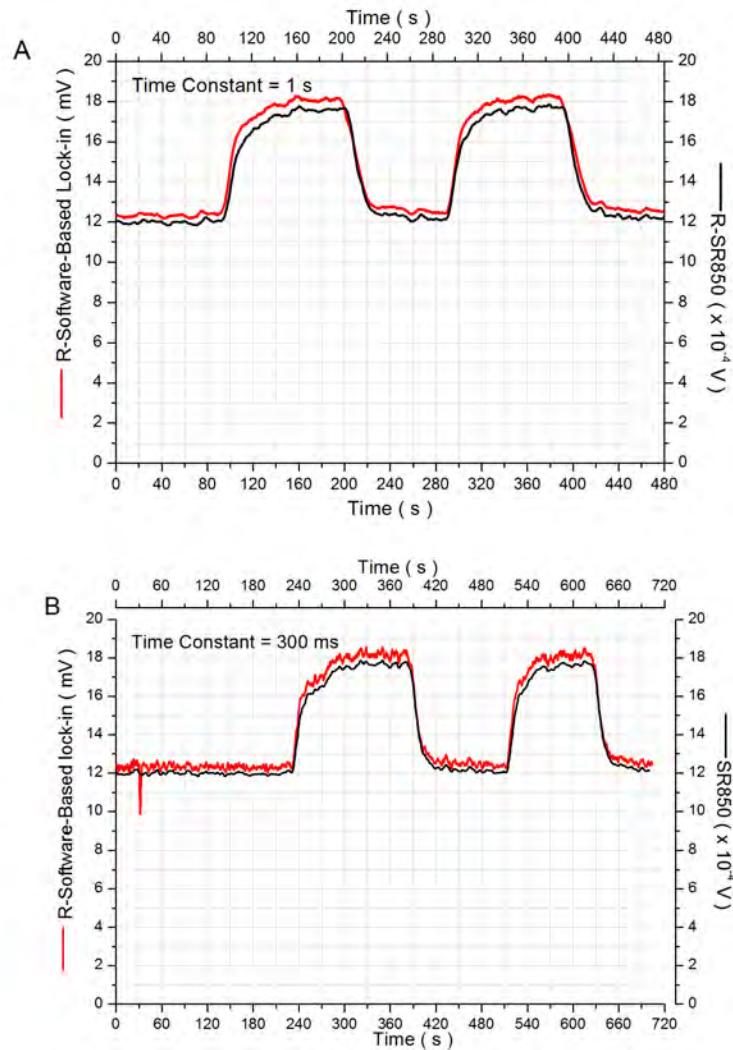
Figure 4.8: Monitoring on the time for the PA signal. The samples were changed from nitrogen (background signal) to ammonia 50 ppm in nitrogen. Diode laser was modulated at same modulation as in figure 4.7.A and 4.7.B.

This lack of synchrony can be clearly seen in figure 4.9, which presents the results for the PA signal, when the diode laser was modulated by wavelength modulation. Figure 4.9 is the amplitude of PA signal. There is a little shift between the spectra. The structure of spectrum for ammonia absorption was preserved and also we can see more details of the lines in the PA signal recovered by virtual software-based lock-in.
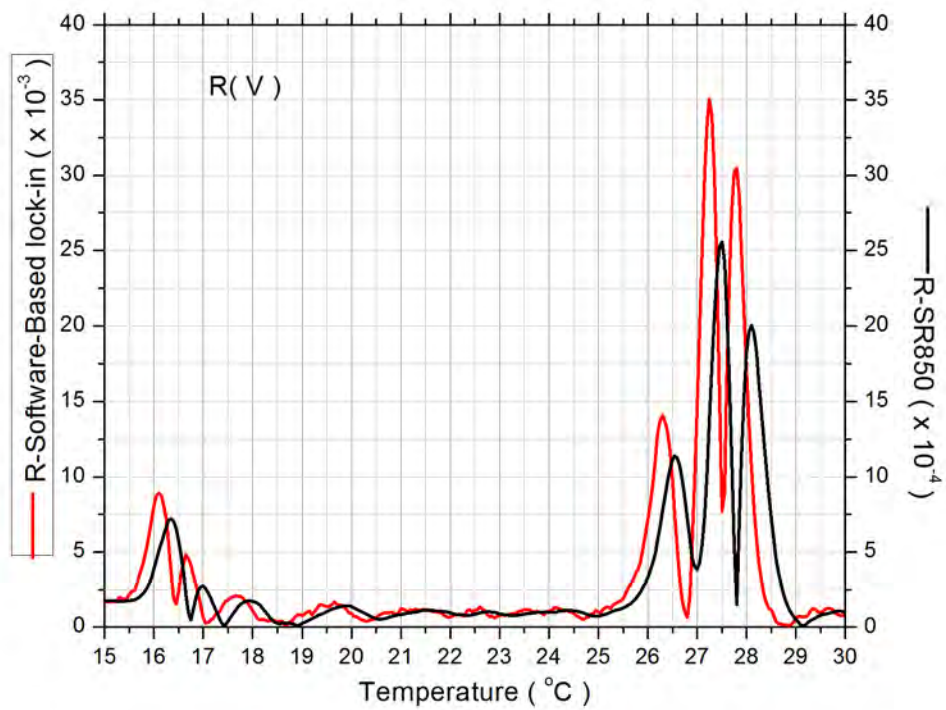
Figure 4.9: Amplitude of PA signal collect from both lock-in. Laser was modulated in wavelength modulation. Laser current was 225 mA modulated by sinus waveform on the resonance frequency of PA cell. Its amplitude was 11 mA.

4.3.2 Dual Quantum Cascade Laser simultaneously modulated for N_2O and NO traces detection in Photoacoustic Spectroscopy

The Figure 4.10 shows the N_2O and NO PA spectra that were measured simultaneously by the using of two quantum cascade lasers and the developed virtual lock-in. The PA signals were generated by exciting a gaseous mixture containing 2.5 ppmV of each chemical species diluted in nitrogen. Two quantum cascade diode lasers were employed. For N_2O spectrum (red line), four absorption peaks were easily identified, being the finger print of N_2O and is in perfect agreement with the spectrum shown in Figure 4.5 obtained by Fast Fourier Transform Infrared (FTIR) - Northwest Infrared Database. Although the measurement was accomplished using a unique sensor (PA cell), the easy identification of the N_2O peaks confirms that the simultaneous detection of N_2O and NO can be carried it out without any influence of one on each other. In the same figure, the spectrum of NO is also shown (green line). Comparing this spectrum with the FTIR spectrum shown in Figure 4.5, similarities are found. However from wavelength higher than $5280\eta m$ any absorption is more observed. This is related to the fact that for such wavelength the intensity of the laser decreases drastically.
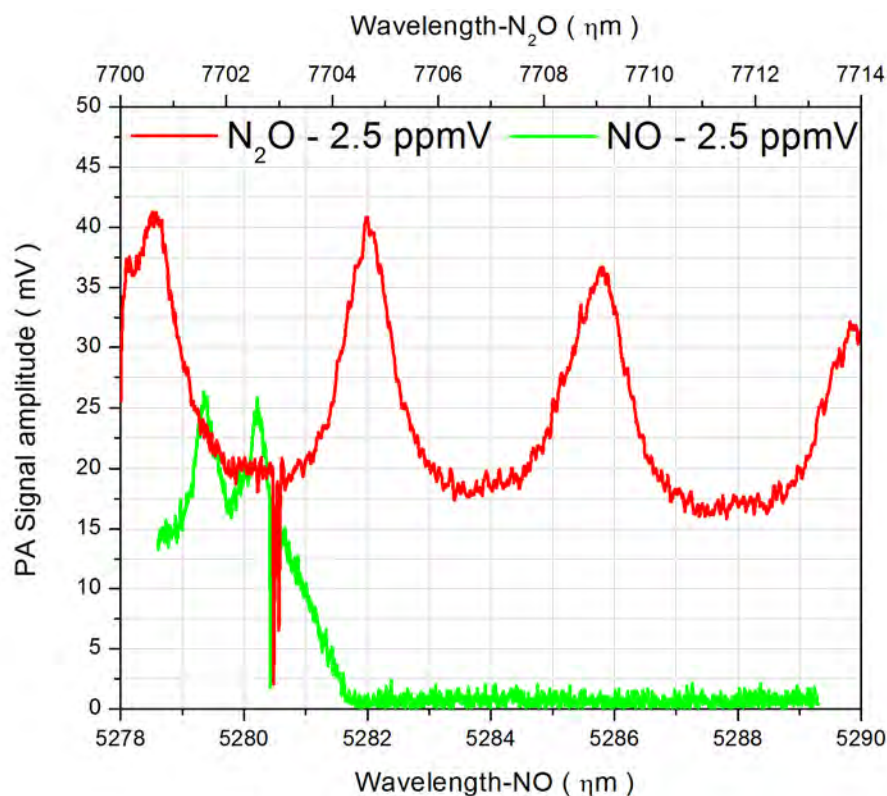
Figure 4.10: Red curve is the absorption spectrum for Nitrous oxide 2.5 ppmV in nitrogen into the emission wavelengths of the QCL. Green curve is the absorption spectrum for Nitric oxide 2.5 ppmV in nitrogen. The spectra were collected simultaneously.

The next step was to see in real time how should be the system behavior during gas exchanging over the time. N_2O and NO (both at 2.5 ppmV in nitrogen) were flowed in the PA cell (red and green curve respectively in the figure 4.11). It can be seen in the figure 4.11, the presence of their individually and independently PA signals. Comparing the PA signal for background and standard sample (2.5 ppmV) for each gas, it looks clear the sensitivity for each one is different. Also, we consider the focus of these results was show a new methodology and the systems were not fine optimized. In the following, both gases were replaced by pure nitrogen using the same flow. It can be observed that the background signal stayed at the same level for both QCL. One more measure nitrous oxide and nitric oxide was made and at the end, pure nitrogen. In this case, we note that the system presented a fast answer, mainly due to the high flow and low adsorption of both gases at PA cell walls, as well as a good repeatability performance.

In the following, a similar procedure to the that described above was carried out, but exchanging the flow of N_2O and NO in an inverse way. Figure 4.12 presents the results for PA signal obtained using this procedure. The PA signal was again monitored over the time and the

QCL temperature remained fixed as described before.
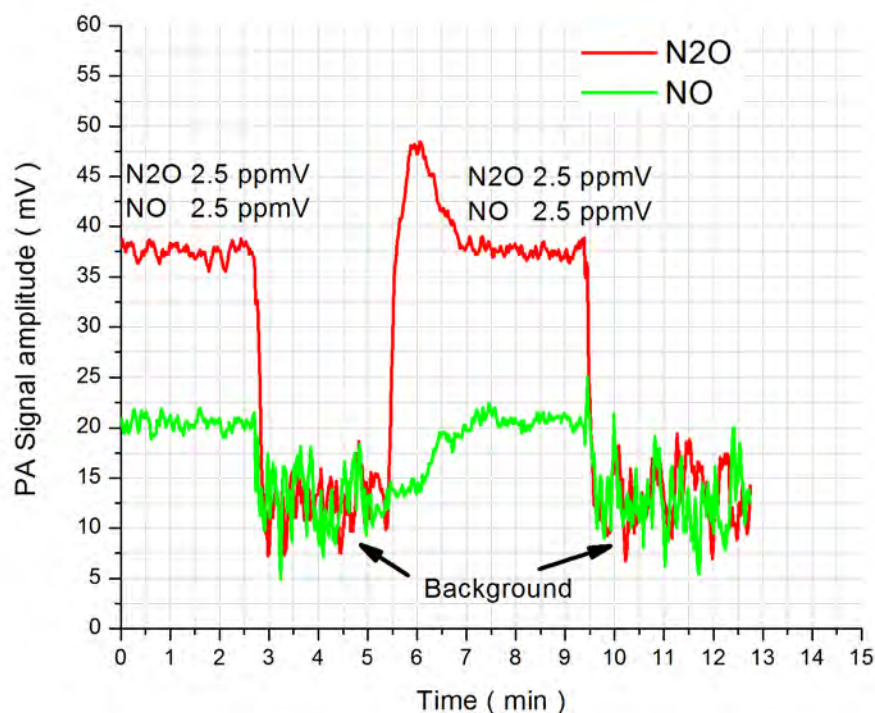
Figure 4.11: Both QCL had the temperature set fixed (-6.6^oC for N_2O QCL and -10^oC for NO QCL). The N_2O and NO flow was interrupted and placed by pure nitrogen flow.

The results presented in the figure 4.12 were obtained for the PA signal using a flow of 100 sccm. The measurement started with pure nitrogen flow (background signal) and was exchanged to 5 ppm of nitrous oxide in nitrogen, five minutes later. It can be observed in the figure 4.12 that the PA signal raises up to $57.5mV$. During these 7 minutes of nitrous oxide flow, as expected it is observed any signal caused by the NO QCL (green curve). After that, again a pure nitrogen flow was used to purge the cell for a few minutes, being replaced by a mixture of 5 ppmV of nitric oxide diluted in nitrogen at a flow of 100 sccm for 2.5 minutes. In the same way as happened for nitrous oxide, nitric oxide could be detected without the influence of nitrous oxide. At last, the cell was filled with pure nitrogen again, in order to reproduce the same background that was observed previously (around $10mV$). One quite interesting issue was the fast response of the PA signal for both gases when filling the cell. A change from background signal to sample signal occurs for a time of 2 minutes. This fast performance of the signal detection could be very important when implementing such trace gas detection system for in vivo samples, as in biological systems.

55
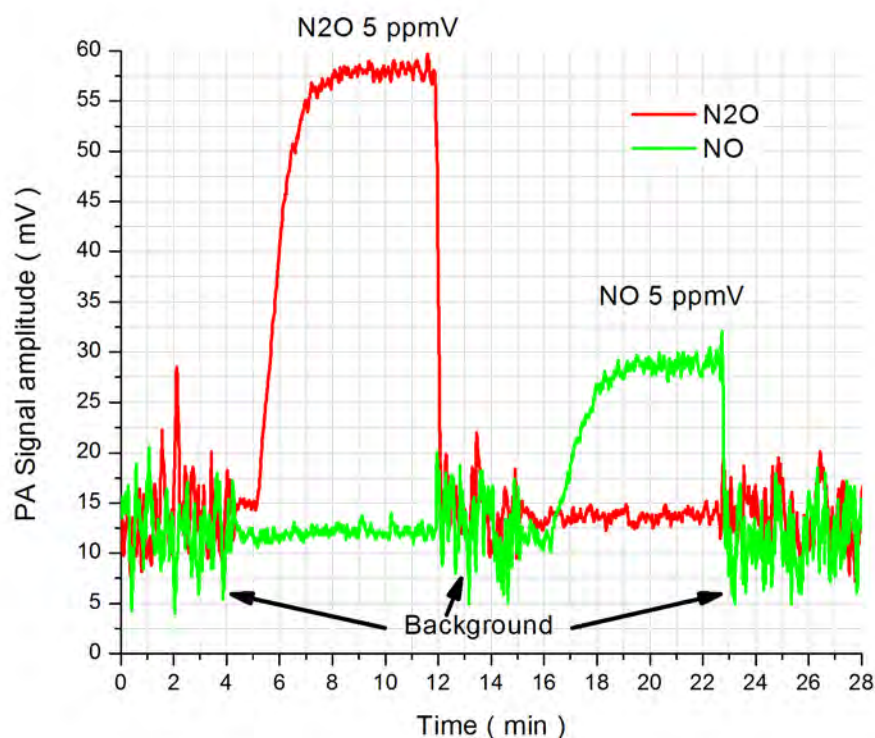
Figure 4.12: The QCLs still in fixed temperature. The flow of NO was stopped and just N_2O 5 ppmV in nitrogen was permitted to flow. After some pure nitrogen flow, NO 5 ppmV in nitrogen was flowed. At the end, pure nitrogen was flowed at the PA cell.

4.4 Conclusion

A software-based lock-in amplifier algorithm was proposed using a DAQ card for two different photoacoustic experimental setups: 1) Ammonia trace detection based on DFB diode laser and 2) two QCLs for simultaneous measurements of two chemical species by using of an unique PA cell. The observed results for the first set up have shown good performance when compared with the results obtained by traditional lock-in amplifier. The quality of spectrum was preserved and all the information about the absorption spectrum are in good agreement with database. The second procedure was quite successful for discriminating individually the absorption spectra of nitric oxide and nitrous oxide. No loss on information was perceived concerning the absorption lines neither any significant interference between the spectra. Additionally, the monitoring of gas concentration over the time shown a good time response using this software-based lock-in. To conclude, the simultaneous dual QCLs system in PA spectroscopy promise a nice outlook for implementing applications in biological systems. This could be espe-

cially important when the experiment involves samples that emit nitrous oxide and nitric oxide or even other molecules, one has to use just an appropriate excitation source.

Chapter 5

Closing

5.1 Conclusion

In this thesis, different experimental setups in photoacoustic spectroscopy based on differential PA cell were used for detecting traces of different chemical species. Specially for ammonia, two different proposals of radiation source were experimented: first, based on Quantum Cascade Laser (QCL) emitting on $9.55\mu m$ and second, based on DFB diode laser emitting on $1531.51\eta m$. Furthermore, a dual QCL system was presented for two chemical species simultaneous traces monitoring ($7.7\mu m$ and $5.29\mu m$), in special, nitric and nitrous oxide.

By using the photoacoustic spectroscopy it was possible to assess the efficiency of three different types of zeolites as nitrogen fertilizers support. The real time and sensitivity by monitoring the ammonia released from zeolites makes the photoacoustic spectroscopy suitable to be employed in studies of kinetic of desorption. Simulating two typical tropical field temperatures (30 and $60^{o}C$), the time evolution of ammonia gas released from Cuban, Chilean and Brazilian sedimentary zeolite (ZC) were measured. Cuban and ZC provided the highest emission rate. While desorption rate for Cuban zeolite and ZC increased respectively by a factor of 6 and 5 as result of the temperature change from 30 to 60°C, the ammonia desorption rate from Chilean samples increased by a factor of about 32. This indicates that an activation temperature higher than 30°C is essential to promote desorption in Chilean zeolite. The fact of the increase ratio of ammonia emission rate for the ZC is close to that obtained for Cuban zeolite is an indication that both zeolites have the same type of adsorption site. It is corroborated by the fact that stilbite is the type of zeolite present in the composition of the ZC.

In order to improve a photoacoustic system for ammonia detection, aiming its field application, a small size photoacoustic cell was developed and a DFB diode laser was used as

excitation source. Such laser has the advantage in the output power (100 mW). Based on this laser, it was made a comparison of performance for two differential PA cells: a traditional design and a smaller version of the traditional design. The results found have shown suitability applications for ammonia and acetylene using this diode laser. In spite of less accuracy in the smaller version, such cell has advantages as fast response and less adsorption in the internal surfaces.

At the end, a system using a software-based lock-in was developed and applied for a simultaneous double QCL setup (The first one to excite nitric oxide traces and second one, to excite nitrous oxide). They were aligned in the same photoacoustic cell and the PA signal respective for each excitation was demodulated. We could conclude the proposed system is suitable for using in PA setups for trace gas detection.

5.2   Outlook

Based on knowledge and experience acquired during the production of this thesis, I would like to suggest further activities about the themes boarded:

- Monitoring the ammonia volatilization rate from different kind of soils placed in Erlenmeyer, sterilized, following official protocols from National Center for Soils Research (Centro Nacional de Pesquisa de Solos, Embrapa Solos) in different urea technologies and physical conditions;

- Development of temperature control system for sweeping temperature up to $500^{o}C$. Such system based on the experimental setup described in the chapter 2 can be used as Ammonia Temperature Programmed Desorption (NH_3TPD) for acidity surface studies.

- Development and tests of a mobile trace gas detection station for monitoring traces of gas from soils in the region of Campos dos Goytacazes. The station would be constituted of DFB diode laser, diode laser controller, data acquisition board, mass flow controllers, power supply, personal computer and program for managing and control, gas pump and photoacoustic cell.

- Monitoring, in real time, the concentrations of traces of ammonia and acetylene using photoacoustic spectroscopy based on DFB diode laser for acetylene absorption ($\lambda = 1531.62\eta m$, 20 mW) and quantum cascade laser for ammonia absorption ($\lambda = 9.53\mu m$,

P = 2 mW) in a dual laser simultaneous detection system from Nitrogen Fixing Bacteria (NFB).

Bibliography

[1] Angelmahr, M., Miklós; A., Hess, P., Wavelength- and amplitude-modulated photoacoustics: comparison of simulated and measured spectra of higher harmonics. Applied Optics, 47(15) (2008), 2806-12.

[2] Arena, F., Dario, R., Parmaliana, A., A characterization study of the surface acidity of solid catalysts by temperature programmed methods, Applied Catalysis A:General, 170 (1998), 127-137.

[3] Baptista-Filho, M., Da Silva, M.G., Sthel, M.S., Schramm, D.U., Vargas, H., Miklós, A., Hess, P., Ammonia detection by using quantum-cascade laser photoacoustic spectroscopy, Applied Optics, 45 (2006), 4966-4971.

[4] Baptista-Filho, M., Da Silva, M.G., Polidoro, J.C., Luna, F.J., Monte, M.B.M., Miklós, A., Souza-Barros, F., Vargas, H., Detection of ammonia released from zeolite by the quantum cascade laser based photoacoustic set-up, Eur. Phys. J. Special Topics, 153 (2008), 547-550.

[5] Bozoki, Z., Szabo, A., Mohacsi, A., Szabo, G., A fully opened photoacoustic resonator based system for fast response gas concentrations measurements, Sensors and Actuators B: Chemical, 147(1), 2010, 206-212.

[6] Claps, R., Englich, F.V., Leleux, D.P., Richter, D., Tittel, F.K., Curl, R.F., Ammonia detection by use of near-infrared diode-laser overtone spectroscopy, Applied Optics, 40(24), 2001, 4387-4394.

[7] Clarkson, P., Esward, T.J., Harris, P.M., Smith, A.A., Smith, I.M., Software simulation of a lock-in amplifier with application fo the evaluation of uncertainties in real measuring systems, Meas. Sci. Technol., 21(4) (2010), 045106.

[8] Costopoulos, D., Miklos, A., Hess, P., Detection of N2O by photoacoustic spectroscopy with a compact, pulsed optical parametric oscillator, APPLIED PHYSICS B, 75(2-3), 385-389, 2002.

[9] Crutzen, P.J., Mosier, A.R., Smith, K.A., Winiwarter, W., N2O release from agro-biofuel production negates global warming reduction by replacing fossil fuels, Atmos. Chem. Phys. Discuss., 7 (2007), 11191-11205.

[10] Curl, R.F., Capasso, F., Gmachl, C., Kosterev, A.A., McManus, B., Lewicki, R., Pusharsky, M., Wysocki, G., Tittel, F.K., Quantum cascade lasers in chemical physics, Chemical Physics Letters, 487(1-3), 1-18, 2010.

[11] Delon, C., Reeves, C.E., Stewart, D.J., Serça, D., Dupont, R., Mari, C., Chaboureau, J.P., Tulet, P., Nitrogen oxide biogenic emissions from soils: impact on NOx and ozone formation in West Africa during AMMA (African Monsoon Multidisciplinary Analysis), Atmos. Chem. Phys. Discuss., 7 (2007), 15155-15188.

[12] Dening, D.C., Simulation of a digital lock-in amplifier, Journal of Magnetic Resonance, 23 (1976), 461-463.

[13] Elia, A., Lugarà, P.M., Di Franco, C., Spagnolo, V., Photoacoustic techniques for trace gas sensing based on semiconductor laser sources, Sensors, 9 (2009), 9616-9628.

[14] Fehér, M., Martin, P.A., Tunable diode laser monitoring of atmospheric trace gas constituents, Spectro. Acta A, 51 (1995), 1579-1599.

[15] Fernholz, T., Teichert, H., Ebert, V., Digital, phase-sensitive detection for in situ diode-laser spectroscopy under rapidly changing transmission conditions, Applied Physics B, 75 (2002), 229-236.

[16] Fischer, M.L., Littlejohn, D., Ammonia at Blodgett Forest, Sierra Nevada, USA, Atmos. Chem. Phys. Discuss., 7 (2007) , 14139-14169.

[17] Garcia-Ruiz, R., Baggs, E.M., N2O emission from soil following combined application of fertilizer-N and ground weed residues, Plant Soil, 299 (2007), 263-274.

[18] Grossel, A., Zeninari, V., Joly, L., Parvitte, B., Courtois, D., Durry, G., New improvements in methane detection using a Helmholtz resonant photoacoustic laser sensor: A compar-

ison between near-IR diode lasers and mid-IR quantum cascade lasers, Spectrochimica Acta Part A, 63(2006), 1021-1028.

[19] Gu J.L., Wang, M., Zhang, X., Thermal-conductivity measurements of polymers by a modified 3w technique, Int. J. Thermophys., 30 (2009), 851-861.

[20] Hansen, T., Trabjergm I., Photoacoustic powder spectra of Ni(II) and Co(II) complexes with aromatic amine N-oxide ligands, Spectrochimica Acta Part A, 54 (1998), 1715-1720.

[21] Hofstetter, D., Beck, M., Faist, J., Nagele, M., Sigrist, M.W., Photoacoustic spectroscopy with quantum cascade distributed-feedback lasers, Optics Letters, 26(12), 887-889, 2001.

[22] Holcomb, M.J., Little, W.A., Cascading lock-in amplification: Application to wavelength modulation spectroscopy, Rev. Sci. Instrum., 63(12) (1992), 5570-5575.

[23] http://www.alpeslasers.com, October 2010.

[24] http://www.anda.gov.br, October 2010.

[25] http://www.fertilizers.org, October 2010.

[26] Imawan, C., Solybacher, F., Steffes, H., Obermeier, E., Gas-sensing characteristics of modifies MoO_3 thin films using Ti-overlayers for NH_3 gas sensors, Sensors and Actuators B, 64, 2000, 193-197.

[27] Kataba, N., Igi, H., Kim, J., Niwa, M., Determination of the Acidic Properties of Zeolite by Theoretical Analysis of Temperature-Programmed Desorption of Ammonia Base don Adsorption Equilibrium, J.Phys.Chem.B, 101 (1997), 5969-5977.

[28] Kosterev, A.A., Tittel, F.K., Chemical sensors based on quantum cascade lasers, EEE JOURNAL OF QUANTUM ELECTRONICS, 38(6), 582-591, 2002.

[29] Kosterev, A., Wysocki, G., Bakhirkin, Y., So, S., Lewicki, R., Fraser, M., Tittel, F., Curl, R.F., Application of quantum cascade lasers to trace gas analysis, Applied Physics B:Lasers and Optics, 90 (2008), 165-176.

[30] Kukla, A.L., Shirshov, Y.M., Piletsky, S.A., Ammonia sensors based on sensitive polyaniline films, Sensors and Actuators b, 37, 1996, 135-140.

[31] Lähdesmäki, I., Lewenstam, A., Ivaska, A., A polypyrrole-based amperometric ammonia sensors, Talanta, 43, 1996, 125-134.

[32] Lähdesmäki, I., Kubiak, W.W., Lewestam, A., Ivaska, A., Interference in a polypyrrole-based amperometric ammonia sensor, Talanta, 52, 2000, 269-275.

[33] Lindley, R.E., Parkes, A.M., Keen, K.A., McNaghten, E.D., Orr-Ewing, A.J., A sensitivity comparison of three photoacoustic cells containing a single microphone, a differential dual microphone or a cantilever pressure sensor, Appl. Phys. B,. 86, 2007, 707-713.

[34] Lundström, I., Spetz, A., Winquist, F., Ackelid, U., Sundgren, H., Catalytic metals and field-effect devices - a useful combination, Sensors and Actuators B, 1(1-6), 1990, 15-20.

[35] Mayo, N., Harth, R., Mor, U., Marouani, D., Hayon, J., Bettelheim, A., Electrochemical response to H_2, O_2, CO_2 and

[36] Miklós, A., et al, Application of acoustic resonators in photoacoustic trace gas analysis and metrology , Rev. Sci. Instrum., 72, 1937, 2001. NH_3 of a solid-state cell based on a cation- or anion-exchange membrane serving as a polymer electrolyte, Anal. Chim. Acta, 310(1), 1995, 139-144.

[37] Miklos, Hess, P., Mohacsi, A., Sneider, J., Kamm, S., Schafer, S., Improved photoacoustic detector for monitoring polar molecules such as ammonia with a $1.53\mu m$ DFB diode laser, AIP Conference Proceedings, 463, 1998, 126-128.

[38] Monte, M.B.M., Middea, A., Paiva, P.R.P., Bernardi, A.C.C., Rezende, N.G.A.M., Baptista-Filho, M., Da Silva, M.G., Vargas, H., Amorin, H.S., Souza-Barros, F., Nutrient release by a Brazilian sedimentary zeolite, Annals of the Brazilian Academy of Sciences, 81(4), 2009, 641-653.

[39] Peng, Y., Zhang, W., Li, L., Yu, Q., Tunable fiber laser and fiber amplifier based photoacoustic spectrometer for trace gas detection, Spectro. Acta A, 74, 924-927, 2009.

[40] Pinder, R.W., Adams, P.J., Ammonia emission controls as a cost-effective strategy for reducing atmospheric particulate matter in the Eastern United States, Environ. Sci. Technol., 41 (2007), 380-386.

[41] Polat, E., Karaca, M., Demir, H., Onus, A.N., Use of Natural Zeolite (Clinoptilolite) in Agriculture, Journal of Fruit and Ornamental Plant Research, 12, 2006, 183-189.

[42] Pushkarsky, M.B., Webber, M.E., Baghdassarian, O., Narasimhan, L.R., Patel, C.K.N., Laser-based photoacoustic ammonia sensors for industrial applications, Appl. Phys. B, 75, 391-396, 2002.

[43] Rabasovic, M.D., Nikolic, M.G., Dramacanin, M.D., Franko, M., Markushev, D.D., Low-cost, portable photoacoustic setup for solid samples, Meas. Sci. Technol., 20 (2009), 095902.

[44] Reháková, M., Cuvanová, S., DziváO, M. , Rimár, J., Gavalóvá, Z., Agricultural and agrochemical uses of natural zeolite of the clinoptilolite type, Current Opinion in Solid State and Materials Science, 8 (2004), 397-404.

[45] Schmohl, A., Miklos, A., Hess, P., Detection of ammonia by photoacoustic spectroscopy with semiconductor lasers, Applied Optics, 41(9), 2002, 1815-1823.

[46] Srivastava, R.K., Lal, P., Dwivedi, R., SrivastatvaS.K., Sensing mechanism in tin oxide-based thick film gas sensors, Sensors and Actuators B, 21, 1994, 213-218.

[47] Terzic, M.,Mozina, J., Horvat, D., Using lasers to measure pollutants, Facta Universitatis: Physics, Chemistry and Technology, 4(1), 2006, 71-81.

[48] Tilman, D., Cassman, K.G., Matson, P.A., Naylor, Polasky, S., Agricultural sustainability and intensive production practices, Nature, 418 (2002), 671-677.

[49] Timmer, B., Olthuis, W., Van den Berg, A., Ammonia sensors and their applications - a review, Sensors and Actuators B, 107, (2005), 666-677.

[50] Tsuboi, T., Hirano, Y., Shibata, Y., Motomiyu, S., Sensitivity improvement of ammonia determination based on flow-injection indophenol spectrophotometry with manganese(II) ion as a catalyst and analysis of exhaust gas of thermal power plant, Anal. Sci., 18, 2002, 1141-1144.

[51] Webber, M.E., MacDonald, T., Pushkarsky, M.B., Patel, C.K.N., Zhao, Y., Nichole M., Mitloehner, F.M., Agricultural ammonia sensor using diode lasers and photoacoustic spectroscopy, Meas. Sci. and Tech., 16, 1547-1553, 2005.

[52] Winquist, F., Spety, A., Lundström, I., Determination of ammonia in air and aqueous samples with a gas-sensitive semiconductor capacitor, Anal. Chim. Acta, 164, 1984, 127-138.

[53] Xu, C.N., Miura, N., Ishida, Y., Matuda, K., Yamazoe, N., Selective detection of NH_3 over NO in combustion exhaust by using Au and MoO_3 doubly promoted WO_3 element, Sensors and Actuators B, 65, 2000, 163-165.

[54] Zakrzewska, K., Mixed oxides as gas sensors, Thin Solid Films, 391, 2001, 229-238.